

Interplay of complete wetting, critical adsorption, and capillary condensation

A. Drzewiński,¹ A. Maciołek,^{2,3,4} A. Barasiński,¹ and S. Dietrich^{2,3}

¹*Institute of Physics, University of Zielona Góra, ul. Prof. Z. Szafrana 4a, 65-516 Zielona Góra, Poland*

²*Max-Planck-Institut für Metallforschung, Heisenbergstrasse 3, D-70569 Stuttgart, Germany*

³*Institut für Theoretische und Angewandte Physik, Universität Stuttgart, Pfaffenwaldring 57, D-70569 Stuttgart, Germany*

⁴*Institute of Physical Chemistry, Polish Academy of Sciences, Department III, Kasprzaka 44/52, PL-01-224 Warsaw, Poland*

(Received 20 August 2008; revised manuscript received 19 January 2009; published 28 April 2009)

The excess adsorption Γ in two-dimensional Ising strips ($\infty \times L$), subject to identical boundary fields at both one-dimensional surfaces decaying in the orthogonal direction j as $-h_1 j^{-p}$, is studied for various values of p and along various thermodynamic paths below the bulk critical point by means of the density-matrix renormalization-group method. The crossover behavior between the complete-wetting and critical-adsorption regimes, occurring in semi-infinite systems, is strongly influenced by confinement effects. Along isotherms $T = \text{const}$ the asymptotic power-law dependences on the external bulk field, which characterize these two regimes, are pre-empted by capillary condensation. Along the pseudo-first-order phase-coexistence line of the strips, which varies with temperature, we find a broad crossover regime in which both the thickness of the wetting film and Γ increase as functions of the reduced temperature τ but do not follow any power law. Above the wetting temperature the order-parameter profiles are not slablike but exhibit wide interfacial variations and pronounced tails.

DOI: [10.1103/PhysRevE.79.041145](https://doi.org/10.1103/PhysRevE.79.041145)

PACS number(s): 05.50.+q, 68.35.Rh, 68.08.Bc

I. INTRODUCTION

Far away from phase boundaries, i.e., deep in the one-phase region, condensed matter is perturbed by confining walls only within a thin layer proportional to the bulk correlation length ξ , i.e., at most approximately 15 Å. This changes drastically if the thermodynamic state of the bulk system is moved toward the boundary of phase transitions between the bulk phases. If the bulk phase transition is of *second* order, the bulk correlation length diverges and so-called critical adsorption occurs; i.e., the perturbation due to the wall located at $y=0$ penetrates deeply into the bulk, resulting in an algebraic divergence of the thickness of the interfacial structure [1,2].

If the bulk phase transition is of *first* order, wetting phenomena occur as a result of a subtle interplay between the substrate potential, interactions among fluid particles, and entropic contributions, in particular interfacial fluctuations [3]. The thickness of the interfacial structure diverges, too, but in this case governed asymptotically by exponents which are determined by the weakest decay exponent of the pair potentials between the fluid particles and of the substrate potential [3].

These two types of phenomena are of significant practical importance ranging from the use of colloidal suspensions [4] to petroleum recovery [5]. Wetting films are relevant in many types of liquid-coating processes, such as lubrication and adhesion [6], and also for microfluidics and nanoprinting [7]. Critical adsorption plays an important role, e.g., for heterogeneous nucleation in supercritical solvents [8] or in micro- and nanofluidic systems in order to achieve wetting of these small structures [9].

A characteristic property of liquids is that first-order gas-liquid or liquid-liquid phase transitions end at critical points. Therefore critical adsorption *must* be replaced by wetting upon moving along a first-order phase boundary. This creates

a puzzle. In the critical region, the coverage Γ , defined as the excess number of fluid particles per area adsorbed on the confining substrate, diverges according to a universal power law. Since liquids governed by dispersion forces (decaying asymptotically $\sim r^{-6}$ with distance r) belong to the Ising universality class [10], which also holds at interfaces, in spatial dimension $d=3$ along the critical isotherm $T=T_c$ one has $\Gamma(\Delta\mu \rightarrow 0) \sim |\Delta\mu|^{-0.194}$ [11], where the undersaturation $\Delta\mu$ measures the deviation of the chemical potential from its value at two-phase coexistence [1,2]. The latter universal singularity is *weaker* than the nonuniversal one, $\Gamma(\Delta\mu \rightarrow 0) \sim |\Delta\mu|^{-1/3}$, for complete wetting [3], although according to general renormalization-group (RG) arguments the dispersion forces, which are responsible for this nonuniversal behavior, at first glance should give rise only to corrections to scaling (i.e., subdominant power laws). Naturally the question arises as to how the system manages to restore universality (i.e., the dominance by the weaker universal power law) upon moving from the nonuniversal complete-wetting behavior to the universal critical-adsorption behavior.

There is also an urgent experimental need to resolve this issue. An ellipsometry study of gravity-thinned complete-wetting layers in the binary-liquid mixture of cyclohexane and methanol [12] reports results which are *not* in accordance with the theoretical predictions. The data indicate the divergence of the film thickness upon approaching the bulk critical temperature characterized by a critical exponent which is distinct from the expected critical exponent for the bulk correlation length. Scaling arguments have been put forward according to which the observed *effective* exponent is associated with a broad intermediate-scaling regime facilitating the crossover from complete wetting in the presence of dispersion forces to critical scaling [12]. Also recent neutron reflectometry data for the adsorption from alkane-perfluoroalkane mixtures at fluorophobic and fluorophilic surfaces [13] are *not* in agreement with the theoretical predictions. These authors have found that the behavior of the

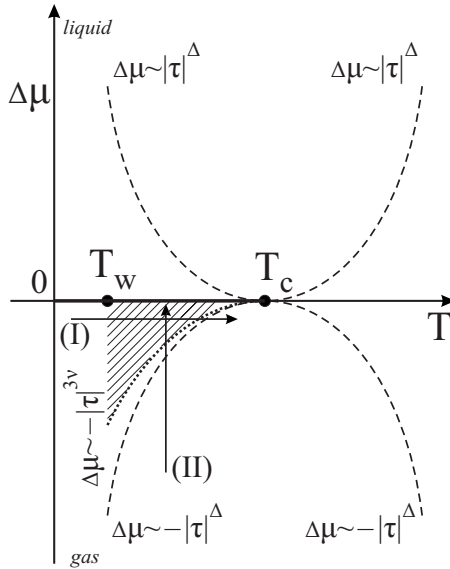


FIG. 1. Schematic drawing of the liquid-gas coexistence curve $\Delta\mu=0$ in the $(\Delta\mu, T)$ bulk phase diagram [11]. The thick solid line indicates the bulk coexistence line. T_w is the transition temperature for a critical-wetting transition. Thermodynamic paths (I) and (II), along which the behavior of the adsorption is discussed in the main text, are displayed as well as various crossover lines. The dashed lines correspond to $\Delta\mu \sim \pm|\tau|^\Delta$ and the dotted line corresponds to $\Delta\mu \sim -|\tau|^{3\nu}$. The hatched area is the complete-wetting regime. Note that $3\nu \approx 1.89$ is larger than $\Delta \approx 1.56$.

adsorption, as a function of temperature in the one-phase region upon approaching liquid-liquid coexistence with the composition well removed from the critical composition, can be represented by a power law with an exponent which differs from both that for complete wetting and that for critical adsorption [13].

The issue formulated above was addressed theoretically in Refs. [11,14,15] and the proposed scenario is such that upon approaching bulk coexistence, i.e., for $\tau \equiv (T-T_c)/T_c$ fixed and $\Delta\mu \rightarrow 0^-$ [see path (II) in Fig. 1], the system will *always* cross over ultimately to the complete-wetting regime but such that upon approaching T_c (i.e., for smaller $|\tau|$), this crossover occurs closer and closer to the coexistence curve. As described more closely in Sec. II, the suggested mechanism is based on the argument that long-ranged dispersion forces are relevant and can dominate if the thickness of the wetting layer is much larger than the bulk correlation length.

So far this proposed scenario, based on general scaling arguments and on the analysis of simple models for the effective interface Hamiltonian (EIH) which are supposed to describe the relevant physics at length scales much larger than the bulk correlation length [11,14], has not been verified satisfactorily by explicit calculations. The main reason is that such calculations require to simultaneously keep track of microscopic details of the system such as the ranges of the interactions as well as of the critical fluctuations near T_c . Theoretical approaches which are geared to capture the microscopic details, such as density-functional theories [14], loose out with respect to the critical fluctuations because they render only mean-field critical exponents. On the other hand,

field-theoretic renormalization-group theory, which can deal successfully with the critical fluctuations, due to its very nature fails to capture the microscopic details. Even if one would be content to deal with the critical phenomena only within mean-field theory (MFT), one would nonetheless miss essential features of the proposed scenario. Mean-field theories of the Landau type correspond to short-ranged interaction with the consequence that the excess adsorptions for both critical adsorption and complete wetting diverge logarithmically and therefore cannot be distinguished. If, instead, one uses density-functional theory incorporating long-ranged interactions one obtains a power law for complete wetting but critical adsorption is still governed by logarithmic singularities. Moreover, due to the inherent mean-field character of the actually available density functionals, they are not able to resolve the difference between the dotted and the dashed line in Fig. 1, because within mean-field theory $\nu=1/2$ and $\Delta=3/2$ so that $3\nu=\Delta$. In Ref. [15] the generalized functional of Fisk and Widom [16] functional that includes long-ranged forces was employed. This functional is consistent with the correct values of the critical exponent but it neglects the capillary-wave-like fluctuations. Therefore a thorough analysis of the proposed scenario requires study a of model for which one can deal fully with both the bulk and surface critical fluctuations of semi-infinite system near T_c as well as with wetting phenomena in the presence of long-ranged forces. This requirement is met by the two-dimensional Ising model ($\nu=1$, $\Delta=15/8$) subject to boundary fields which decay algebraically with various choices of the decay exponent p .

Moreover, there is a recent experimental interest in such genuine two-dimensional systems in the context of proteins immersed in a fluid two-component lipid membrane which is near phase separation, including a critical point belonging to the $d=2$ Ising universality class [17,18]. If two such proteins are close to each other the structural properties of the membrane between them can be described in terms of the strips studied here, giving even rise to interesting effective interactions between the proteins.

For the $d=2$ Ising model exact results for critical wetting with short-ranged forces [19] and for critical adsorption [20] are available. However, in the presence of long-ranged boundary fields and for complete wetting, which requires study of thermodynamic states off bulk coexistence, one has to resort to numerical techniques or Monte Carlo simulations. For both these methods the confinement of the system is unavoidable, which complicates the aforementioned crossover behavior due to finite-size effects. Depending on the type of boundary conditions also other phenomena, such as capillary condensation, can occur. However, one may expect that for sufficiently large systems the finite-size effects should be small and that the actual leading asymptotic behavior can be reached.

The application of the density-matrix renormalization-group (DMRG) method in $d=2$ [21–24] provides essentially exact numerical results for strips which are infinitely long in one direction and have widths up to $L=700$ lattice constants in the other direction. It allows one to study arbitrary boundary and bulk fields. The comparison with exact results for critical wetting transitions in the case of a vanishing bulk

field and in the presence of contact surface fields shows that the DMRG method provides a very high accuracy for a broad range of temperatures. Using this method, confinement effects on critical adsorption [25] and complete wetting [26] in the $d=2$ Ising model have been studied before. We employ the DMRG method to investigate systematically the adsorption properties along various thermodynamic paths and thus we test the aforementioned predictions of the mesoscopic effective interface Hamiltonian approaches for boundary fields decaying in the orthogonal direction j from the surface as $-h_{1j}j^{-p}$, with $p=1.5, 2, 3, 4$, and 50 . For $p < 3$ our preceding work [27] showed that the quasiexact calculations for the full microscopic $2d$ Ising model reveal results which are not captured by simple effective interface models describing wetting phenomena. Therefore for this range of decay exponents the interplay of complete wetting and critical adsorption can potentially show rather unexpected features, which will be indeed the case.

Our analysis shows, which is rather surprising, that the leading asymptotic behavior for complete wetting, predicted from effective interface Hamiltonian models, cannot be reached even for strips as wide as $L=700$. Inevitably, one therefore encounters the interplay between complete wetting, critical adsorption, and capillary condensation. The interplay of these three phenomena has not been discussed before, although it might be also relevant for adsorption-induced colloidal aggregation in binary-liquid mixtures [28,29]. We note that, because our studies deal with two-dimensional systems, they cannot provide a quantitative explanation of the experiments described above.

The paper is organized as follows. In Sec. II theoretical predictions for semi-infinite systems are summarized and the predictions for the crossover behavior are described in detail. In Sec. III we introduce the microscopic model and the method. Numerical results for the phase diagram of the present model are described in Sec. IV. Results for the magnetization profiles, the thicknesses of wetting layers, and the adsorption along the isotherms and along the line of pseudo-phase-coexistence are reported in Sec. V. In Sec. VI we summarize our results and draw our conclusions.

II. DESCRIPTION OF SEMI-INFINITE SYSTEMS

A useful global characterization of the interfacial structure near a single wall is provided by the coverage Γ defined as the excess number of fluid particles per area adsorbed on the confining substrate:

$$\Gamma = \int_0^{\infty} [\rho(y) - \rho_b] dy, \quad (1)$$

where ρ_b is the bulk number density for a given temperature T and chemical potential μ . Here the fluid number density profile $\rho(\mathbf{r}) \equiv \rho(y)$ is assumed to vary only in the direction y normal to the wall located at $y=0$.

A. Complete wetting

If the substrate potential is sufficiently strong, there is a wetting transition temperature T_w such that if the bulk gas phase approaches gas-liquid coexistence $\mu_0(T)$ along iso-

therms at temperatures $T > T_w$, Γ diverges due to complete wetting; i.e., a macroscopically thick wetting film is formed. The equilibrium thickness ℓ_0 of the wetting film can be defined as

$$\ell_0 = \Gamma / (\rho_l - \rho_g), \quad (2)$$

where ρ_l and ρ_g are the bulk number densities of the liquid and gas phases, respectively, at coexistence. In magnetic language the fluid is an Ising ferromagnet, the gas phase corresponds to the spin-down phase, the liquid phase corresponds to the spin-up phase, and the difference between the substrate potential and its analog for fluid-fluid interactions corresponds to a surface field. The undersaturation $\Delta\mu = [\mu - \mu_0(T)] / k_B T_c$ is proportional to the bulk field H .

In the complete-wetting regime the increase in the adsorption upon approaching bulk coexistence can be described as [3]

$$\Gamma(\Delta\mu \rightarrow 0, T) \sim |\Delta\mu|^{-\beta_s^{co}}, \quad T_w < T < T_c. \quad (3)$$

The exponent β_s^{co} for this surface quantity depends on the form of the fluid-fluid and substrate-fluid forces as well as on the spatial dimension d . In $d=3$, β_s^{co} is nonuniversal; $\beta_s^{co} = 0$ (i.e., $\sim \ln \Delta\mu$) for short-ranged forces, whilst $\beta_s^{co} = 1/p$ for wall-fluid and fluid-fluid pair potentials decaying as $r^{-(d+p)}$ ($p=3$ for nonretarded dispersion forces). Because the upper critical dimension for complete wetting with long-ranged forces is $d_s^* = 3 - 4/(p+1) < 3$ [3,30,31], these mean-field exponents $\beta_s^{co} = 1/p$ are not altered by interfacial fluctuations. For short-ranged forces, i.e., $p \rightarrow \infty$, one has $d_s^* = 3$ so that fluctuations matter in $d=3$, but it turns that for complete wetting they change only the amplitude of the thickness of wetting film [3].

In $d=2$ interfacial fluctuations in the wetting films are much stronger and $2 = d < d_s^*$ for both short-ranged and dispersion forces ($p=4$ for the latter in $d=2$). Accordingly the complete-wetting exponent takes a universal value which turns out to be given by $\beta_s^{co} = 1/3$, provided $p \geq 3$ so that interfacial fluctuations dominate [30,31]. From the point of view of an effective interface Hamiltonian, this latter universality of β_s^{co} is due to the entropic effects of the fluctuating, unbinding interface which give rise to an effective repulsive interaction for the gas-liquid interface, taken to be located on average at $y=\ell$, which decays $\sim \ell^{-\kappa}$ with $\kappa = 2(d-1)/(3-d)$; $\kappa(d=2)=2$. If this entropic repulsion dominates the effective interaction contribution $\sim \ell^{-(p-1)}$, i.e., if $p > \kappa + 1$, one finds $\beta_s^{co} = 1/3$ in $d=2$. This defines the so-called weak-fluctuation regime for complete wetting. According to this argument, for $p < 3$ one has instead $\beta_s^{co} = 1/p$.

The considerations leading to the above predictions are valid only if the equilibrium wetting film thickness ℓ_0 is much larger than the bulk correlation length ξ , i.e., $\ell_0 \gg \xi$.

B. Critical adsorption

Near a critical point T_c , a confining wall generically provides an effective surface field h_1 acting on the order parameter (OP) $m(y) \equiv [\rho(y) - \rho_c] / \rho_c$, where ρ_c is the critical density, describing the continuous phase transition and leading to the so-called critical adsorption [1-3,32,33].

Specifically, along bulk coexistence $\Delta\mu=0$ one has asymptotically

$$\Gamma \sim |\tau|^{\beta-\nu}, \quad \Delta\mu=0, \quad (4)$$

whereas along the path $\tau=0$

$$\Gamma \sim |\Delta\mu|^{(\beta-\nu)/\Delta}, \quad (5)$$

where ν , β , and Δ are standard bulk critical exponents.

We note that both Eqs. (4) and (5) are consistent with the scaling behavior of $\Gamma \sim m\xi$ due to

$$\xi_{\pm}(\tau, \Delta\mu) = |\tau|^{-\nu} \Xi_{\pm}(\Delta\mu |\tau|^{-\Delta}), \quad (6)$$

where Ξ_{\pm} are scaling functions above (+) and below (−) T_c . Since $\Xi_{\pm}(0) = \text{const} = \xi_0^{\pm}$ one has

$$\xi_{\pm}(\tau, 0) = \xi_0^{\pm} |\tau|^{-\nu}, \quad (7)$$

and $m \sim |\tau|^{\beta}$ for $\delta\mu=0$. On the other hand $\Xi_{\pm}(x \rightarrow \pm\infty) \sim |x|^{-\nu/\Delta}$ and thus at $\tau=0$

$$\xi(0, \Delta\mu) = \xi_0^{(\mu)} |\Delta\mu|^{-\nu/\Delta} \quad (8)$$

and $m \sim |\Delta\mu|^{1/\delta}$, with $\delta = \Delta/\beta$. Within MFT $\beta = \nu = 1/2$ which results in a logarithmic divergence along both paths.

Equation (5) is expected to hold [11] also below T_c for $|\Delta\mu| \gg |\tau|^{\Delta}$ on both the wetting and nonwetting sides of the coexistence curve, i.e., if the argument of the scaling functions Ξ_{\pm} approaches infinity so that the behavior of ξ_{\pm} is governed by $\Delta\mu$ [Eq. (8)]. This regime is referred to as the *critical-adsorption regime*. Similarly, above T_c Eq. (4) is expected to be valid within the regime $|\Delta\mu| \ll |\tau|^{\Delta}$, i.e., where the behavior of ξ is governed by τ [Eq. (7)]. The same should hold close to bulk coexistence below T_c . However, it has been argued [11,12,14] that even near the critical point long-ranged forces are important, in the sense that for τ fixed and $\Delta\mu \rightarrow 0^-$ the system will *always* cross over to the complete-wetting regime [Eq. (3)], although upon approaching T_c (i.e., for smaller τ) this crossover will occur closer and closer to the coexistence curve. The expectation for this scenario to hold is based on the argument that long-ranged forces are relevant and thus dominant for $\ell_0 \gg \xi$. Since $\ell_0 \sim |\Delta\mu|^{-\beta_s^{co}}$ and $\xi \sim |\tau|^{-\nu}$, this leads to the condition $|\Delta\mu| \ll |\tau|^{\nu/\beta_s^{co}}$; i.e., $|\Delta\mu| \ll \tau^{3\nu}$ for dispersion forces in $d=3$. Thus on the gas-side region between the coexistence curve $\Delta\mu=0$ and the curve $\Delta\mu = \text{const} \times |\tau|^{\nu/\beta_s^{co}}$, the adsorption should be governed by complete-wetting phenomena, whereas the divergence of the adsorption $|\tau|^{\beta-\nu}$ according to Eq. (4) should be limited to the range $|\Delta\mu|^{1/\Delta} \ll |\tau| \ll |\Delta\mu|^{\beta_s^{co}/\nu}$. Furthermore, the effective interface Hamiltonian approach predicts that contrary to the critical-adsorption regime, in the wetting-dominated region the divergence of Γ should depend on the choice of the thermodynamic path taken. In particular, for any isotherm within this regime one expects $\Gamma \sim |\Delta\mu|^{-\beta_s^{co}}$, but along a path $\Delta\mu = \text{const} |\tau|^x$ with $x > \nu/\beta_s^{co}$ one expects $\Gamma \sim |\tau|^{\beta-x\beta_s^{co}}$. This follows from Eq. (2) with $\Delta\rho \sim |\tau|^{\beta}$ and $\ell_0 \sim |\Delta\mu|^{-\beta_s^{co}}$.

C. Crossover phenomena

These regimes described above are expected to give rise to rich crossover phenomena for the adsorption $\Gamma(\Delta\mu, T)$

upon crossing boundary lines between them along various thermodynamic paths. Two of them are particularly relevant for the present work: (i) isotherms $T = \text{const} < T_c$ with $\Delta\mu \rightarrow 0^-$ [see path (II) in Fig. 1] and (ii) a path parallel to the coexistence curve on the gas side with a small undersaturation $\Delta\mu = \text{const} < 0$ and with $T \rightarrow T_c$ [path (I) in Fig. 1].

Along an isotherm $T = \text{const} > T_w$ and below the curve $\Delta\mu \sim -|\tau|^{\Delta}$ (see Fig. 1) Γ increases as $|\Delta\mu|^{(\beta-\nu)/\Delta}$ upon approaching bulk coexistence from the gas side, i.e., for decreasing $|\Delta\mu|$, until one enters the crossover region between the lines $\Delta\mu = -\text{const} |\tau|^{\Delta}$ and $\Delta\mu = -\text{const} |\tau|^{\nu/\beta_s^{co}}$ in which Γ increases further; but therein no specific and well-defined power law can be expected. Finally, when the path crosses the curve $\Delta\mu = -\text{const} |\tau|^{\nu/\beta_s^{co}}$ it enters the regime governed by wetting phenomena so that the adsorption should diverge as $|\Delta\mu|^{-\beta_s^{co}}$. For $\mu = \mu_0$ the wall is wet and the adsorption is infinite (provided $T_w < T \leq T_c$).

The behavior of the adsorption along a path parallel to the coexistence curve is expected to be equally rich. Let us consider the case that the wetting transition at coexistence is continuous at $T = T_w$. According to the theory of wetting phenomena [3] the adsorption Γ increases smoothly to some finite value (because $|\Delta\mu| > 0$) upon approaching the wetting temperature T_w . This increase is governed by the scaling laws with respect to $\Delta\mu$ and τ which are associated with critical wetting. Upon a further increase in the temperature the adsorption should slightly decrease because $\Gamma = \ell_0 \Delta\rho$, with $\ell_0 = \text{const}$, due to $\Delta\mu = \text{const}$, and $\Delta\rho = \rho_l - \rho_g \sim |\tau|^{\beta}$ until the crossover line $\Delta\mu = -\text{const} |\tau|^{\nu/\beta_s^{co}}$ to the critical-adsorption regime is reached. There Γ should increase $\sim |\tau|^{\beta-\nu}$ until the next crossover line $\Delta\mu = -\text{const} |\tau|^{\Delta}$ is encountered, beyond which Γ as a function of τ should saturate at a certain large value $\sim |\Delta\mu|^{(\beta-\nu)/\Delta}$. Finally, after passing the right branch of the crossover line $\Delta\mu \sim -\tau^{\Delta}$ (above T_c), the adsorption should decrease $\sim \tau^{\beta-\nu}$ upon increasing τ .

III. MICROSCOPIC MODEL

In this section we introduce the microscopic model within which we investigate quantitatively the crossover regimes described above. Specifically, we consider an Ising ferromagnet on a square lattice, with the lattice spacing set to 1, of size $M \times L$, with $M \rightarrow \infty$ (strip geometry) subject to identical boundary fields. At each site, labeled (k, j) , there is an Ising spin variable taking the value $\sigma_{k,j} = \pm 1$. The boundary surfaces are located in the rows $j=1$ and $j=L$. We assume periodic boundary conditions (PBCs) in the lateral x direction. Our model Hamiltonian for the strip with PBCs and $M \rightarrow \infty$ is given by

$$\mathcal{H} = -J \left(\sum_{\langle kj, k'j' \rangle} \sigma_{j,k} \sigma_{j',k'} + \sum_{j=1}^L V_{j,L}^{ext} \sum_k \sigma_{k,j} + H \sum_{k,j} \sigma_{k,j} \right), \quad (9)$$

where the first sum is over all nearest-neighbor pairs. The external potential experienced by a spin in the row j is the sum of the two independent wall contributions: $V_{j,L}^{ext} = V_j^s + V_{L+1-j}^s$. It is measured in units of $J > 0$. The single-boundary field V_j^s is assumed to have the form

$$V_j^s = \frac{h_1}{j^p}, \quad (10)$$

with $p > 0$ and $h_1 > 0$. H is a bulk magnetic field. According to Eq. (9) h_1 and H are dimensionless.

Using the equivalence between the lattice gas and the Ising model (see, e.g., Ref. [34]), this model can be viewed as being obtained from a $2d$ lattice gas model mimicking a two-dimensional one-component fluid with a short-ranged interaction potential between the fluid particles and either short-ranged or long-ranged substrate potentials. This analogy can be extended to binary-liquid mixtures [35].

We recall that although there is no longer any true phase transition for finite L , in two-dimensional Ising strips with large L there is still a line of only extremely weakly rounded first-order transitions ending at a pseudocritical point the location of which in the plane (H, T) spanned by the bulk field and the temperature T depends on the character of the surface fields [36,37]. For surfaces which prefer the same bulk phase, the phenomenon equivalent to capillary condensation takes place. The pseudo-phase-coexistence between phases of spin-up and spin-down occurs along a line $H_{ca}(T, L)$, which is given approximately by the analog of the Kelvin equation [38]:

$$H_{ca}(T, L) \approx -\sigma(T)/[L|m_b^{(0)}(T)|], \quad (11)$$

where $\sigma(T)$ is the interfacial tension (divided by J) between the coexisting bulk phases and $m_b^{(0)}(T) < 0$ is the spontaneous bulk magnetization for $H=0^-$. For the $d=2$ Ising model, the surface tension is given exactly by $\beta J \sigma(T) = 2(K - K^*)$, where $K = J/k_B T$, $K^* = \text{arth}[\exp(-2K)]$, and $K_c = J/k_B T_c = \ln(1 + \sqrt{2})$ [39].

The occurrence of thick wetting films of up-spins (+) at the two surfaces, for a thermodynamic bulk state corresponding to down-spins (-), gives rise to nontrivial corrections to Eq. (11) which shift the condensation line to larger values of $|H|$ [37,40]. The pseudo-coexistence line ends at a pseudocapillary critical point $(H_{c,L}, T_{c,L})$, where $T_{c,L}(h_1, p)$ lies below the temperature T_c of the bulk critical point. Its position as well as that of $H_{c,L}$ depends on L as well as on the strength and the range of the surface fields. For large L and strong h_1 the shifts of the critical temperature and of the bulk field $H_{c,L}(h_1, p)$ are given by [37,41,42] (see Fig. 2)

$$T_{c,L} - T_c \sim -L^{-1/\nu}, \quad H_{c,L} \sim -L^{-\Delta/\nu}, \quad (12)$$

with $\nu=1$ and $\Delta=15/8$ for the two-dimensional Ising model.

IV. PHASE DIAGRAM

In Fig. 3 we show the phase diagram for the present model calculated by using the DMRG method for a strip of width 340 with $h_1=0.8$ and three choices of the parameter p describing the decay of the boundary field: $p=50, 3$, and 2 . The case $p=50$ is expected to resemble the behavior corresponding to short-ranged surface forces [25(d)]. In this figure we display the various crossover lines discussed in Secs. I and II and the thermodynamic paths along which we have calculated the adsorption Γ . The pseudo-phase-coexistence

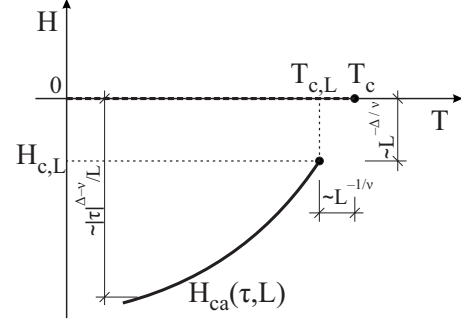


FIG. 2. Scaling behavior of the capillary condensation line $H_{ca}(\tau, L)$ near bulk criticality ($T=T_c$, $H=0$). For $\tau=(T-T_c)/T_c \neq 0$ and $L \rightarrow \infty$, $H_{ca}(\tau, L)$ approaches bulk coexistence $H=0$ (dashed line) as $|\tau|^{\Delta-\nu}/L$ and the capillary critical point $(T_{c,L}, H_{c,L})$ approaches T_c and $H=0$ as $L^{-1/\nu}$ and $L^{-\Delta/\nu}$, respectively. The latter is valid for strong surface field. It takes the form $L^{-(\Delta-\Delta_1)/\nu}$, where Δ_1 is the surface gap exponent, for weak h_1 [42]. Here $T_{c,L} < T_c$. Note the upward bent of the capillary condensation line; this feature is due to $\Delta - \nu < 1$ [see, cf. the text following Eq. (14)]. However, this bent is weak: $\Delta - \nu = 7/8 = 0.875$ in $d=2$ and $\Delta - \nu = 0.936$ in $d=3$.

line, the crossover lines, and the adsorption have been determined for $2d$ Ising strips within the DMRG method.

The thick solid line in Fig. 3 indicates the bulk phase-coexistence line ($H=0$, $T < T_c$) terminating at the bulk critical point ($H=0$, $T=T_c \approx 2.269 J/k_B$). The symbols (open circles for $p=2$, open squares for $p=3$, and stars for $p=50$) show the pseudo-phase-coexistence. It turns out that the

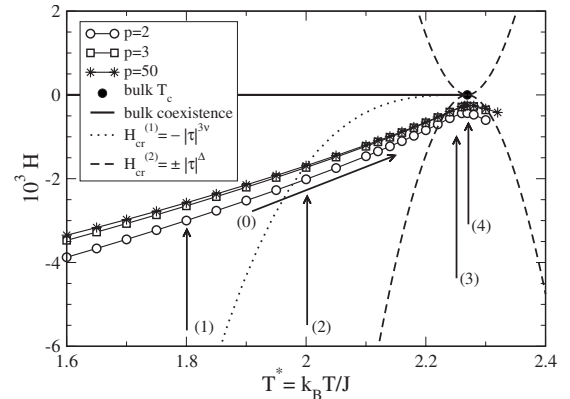


FIG. 3. Phase diagram for a $d=2$ Ising strip subject to identical boundary fields V_j^{ext} [see Eq. (10)] obtained by using DMRG for a strip width $L=340$ and the amplitude $h_1=0.8$ for the boundary fields. The thick solid line indicates the bulk coexistence line at $H=0$. The lines interpolating the symbols represent the pseudo-phase-coexistence lines $H_{ca}(T, L; p)$ for three different values of the exponent p governing the algebraic decay of the boundary fields: open circles correspond to $p=2$, open squares correspond to $p=3$, and stars correspond to $p=50$. Various crossover lines $H_{cr}^{(1)} = -|\tau|^{3\nu}$ and $H_{cr}^{(2)} = \pm|\tau|^\Delta$ are shown with $\nu=1$ and $\Delta=15/8$ in $d=2$, as discussed in the main text, as well as thermodynamic paths (1)–(4) along which the adsorption has been calculated. (1)–(4) are various isotherms and (0) runs parallel to the pseudo-coexistence line. Thus path (0) resembles [in a certain sense (see later)] a path of type (I) in Fig. 1, whereas paths (1)–(4) do correspond to a path of type (II) in Fig. 1.

pseudo-phase-coexistence line for long-ranged boundary fields is located slightly farther away from the bulk coexistence line, especially at lower temperatures, than the pseudo-phase-coexistence line for the short-ranged boundary fields ($p=50$). These pseudolines have been identified as those positions (H, T) in the phase diagram where the total magnetization of the strip vanishes, i.e., $\sum_{j=1}^L m_j = 0$, with $m_j = \langle \sigma_{k,j} \rangle$. As can be seen in Fig. 3, for $T < T_c$ ($T > T_c$) the line defined by the zeros of the total magnetization moves to less (more) negative values of H upon increasing T . Determining $T_{c,L}$ for different values of p and L is beyond the scope of the present analysis.

We have found that one can clearly distinguish two different regimes for the behavior of the pseudo-phase-coexistence line, which are separated by a crossover region occurring for $1 \lesssim p \lesssim 3$. In both of these two regimes the shift $H_{ca}(T, L; p) - H_{ca}(T, L; \infty)$ varies exponentially but with different decay constants. [We note that $p = \infty$ corresponds to a pure surface contact field at $j=1, L$; see Eq. (10).] For $p \leq 1$ the shift of $H_{ca}(T, L; p)$ relative to the short-ranged pseudo-phase-coexistence line does not depend on the temperature.

We have also analyzed the aforementioned scaling behavior of the pseudo-phase-coexistence line of capillary condensation $H_{ca}(T, L; p)$. For $\tau \neq 0$ the capillary condensation line $H_{ca}(\tau, L)$ is expected [43] to approach the bulk coexistence line $H=0$ as $1/L$ for $L \rightarrow \infty$ in accordance with the Kelvin equation [Eq. (11)]. Near T_c , i.e., for $|\tau| \ll 1$, scaling arguments lead to the scaling behavior [see Eqs. (6) and (7)]:

$$H_{ca}(\tau, L) = |\tau|^{\Delta} \tilde{g}(L/\xi, h_1 |\tau|^{-\Delta_1}), \quad (13)$$

where Δ_1 is the surface gap exponent [$\Delta_1(d=2)=1/2$] due to the presence of surface fields [2]; note that $\tilde{g} < 0$. [In Eq. (13) the scaling of h_1 holds if p is sufficiently large, i.e., $p > 15/8$; see the text preceding, cf. Eq. (16).] Since ξ depends on $\Delta\mu$ [see Eq. (6)], in Eq. (13) the first scaling variable of \tilde{g} depends also on $H_{ca}(\tau, L)$, rendering an implicit equation for $H_{ca}(\tau, L)$. To leading order $H_{ca}(\tau, L)$ is given by Eq. (13) with ξ from Eq. (7). In the following h_1 is considered to be large enough so that $\tilde{g}(x, u \rightarrow \infty) = g(x) < 0$ becomes independent of the second scaling variable. The analytic property $g(x \rightarrow \infty) \sim 1/x$ renders $H_{ca}(\tau, L \rightarrow \infty) \sim |\tau|^{\Delta-\nu}/L$ for $\tau \neq 0$ fixed and $L \rightarrow \infty$, in accordance with the Kelvin equation. On the other hand, for L fixed and $\tau \rightarrow 0$ one has $g(x \rightarrow 0) \sim x^{-\Delta/\nu}$ (see below), which ensures that the limit $\tau \rightarrow 0$ renders a nontrivial function of L : $H_{ca}(\tau \rightarrow 0, L) \sim L^{-\Delta/\nu}$, with $\Delta/\nu = 15/8$ in $d=2$. For weak surface fields $H_{ca}(\tau, L) \sim h_1 |\tau|^{\Delta-\Delta_1} \tilde{g}(L/\xi)$, with $\tilde{g}(x \rightarrow 0) \sim x^{-(\Delta-\Delta_1)/\nu}$, $\tilde{g} < 0$, so that $H_{ca}(\tau \rightarrow 0, L) \sim L^{-(\Delta-\Delta_1)/\nu}$ [42].

The capillary condensation line ends at a capillary critical point, at which the free energy of the confined system expressed in terms of the scaling variables ($L/\xi, H|\tau|^{-\Delta}$) is singular at a point (x_0, y_0) , implying Eq. (12), which is consistent with the scaling behavior $H_{ca}(\tau, L \rightarrow \infty) \sim |\tau|^{\Delta-\nu}/L$. This scaling behavior of the capillary condensation line is sketched in Fig. 2.

With $\xi \sim |\tau|^{-\nu}$ [see Eq. (6)] the scaling form for the capillary condensation line can be written equivalently as

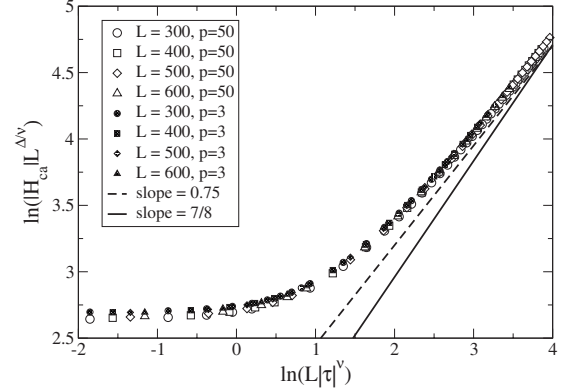


FIG. 4. The log-log plot of the scaling function $\hat{g}(x=L/\xi)$ [see Eq. (14)] of the capillary condensation line $H_{ca}(\tau, L)$ calculated for several large values of L and for a short-ranged ($p=50$) and a long-ranged ($p=3$) boundary field. In the limit $x \equiv L|\tau|^\nu \rightarrow 0$ the scaling function saturates at a constant nonzero value, whereas $\hat{g}(x \rightarrow \infty) \sim x^w$, with $w \approx 0.75$. The expected value $(\Delta-\nu)/\nu = 7/8 = 0.875$ is not yet reached.

$$H_{ca}(\tau, L) = L^{-\Delta/\nu} \hat{g}(L/\xi), \quad (14)$$

where $\hat{g}(x) = x^{\Delta/\nu} g(x) < 0$. We test to which extent scaling holds for the present model with $p=50$ and $p=3$ by plotting $|H_{ca}|L^{\Delta/\nu}$ versus $L|\tau|^\nu$ for several strip widths L . Although we neglect the H dependence of ξ [see above and compare Eq. (6)], the data collapse is very good. From the log-log plot (see Fig. 4) one can see that $\hat{g}(x \rightarrow 0) = \text{const}$, which implies $g(x \rightarrow 0) \sim x^{-\Delta/\nu}$ (see above) and $H_{ca}(0, L) \sim L^{-\Delta/\nu}$. In the limit $x \gg 1$ our data fit very well to a power law $\hat{g}(x \rightarrow \infty) \sim x^w$, with the effective exponent $w \approx 0.75$; w is smaller than the value $(\Delta-\nu)/\nu = 7/8 = 0.875$ which would lead to the predicted behavior $H_{ca}(\tau, L \rightarrow \infty) \sim |\tau|^{\Delta-\nu}/L$. One might be inclined to put the blame for the fact that w has not yet reached this expected asymptotic value on corrections caused by the aforementioned H dependence of the bulk correlation length, according to which Eq. (14) reads $H_{ca}(\tau, L)L^{\Delta/\nu} = \hat{g}(L|\tau|^\nu [\Xi(H_{ca}|\tau|^{-\Delta})^{-1}])$ [see Eq. (6)]. This additional dependence actually spoils the scaling in terms of the scaling variable $x=L|\tau|^\nu$. Since, however, scaling is observed, the latter dependence must be weak and the too small value of the exponent w must be due to other corrections, possibly due to the presence of the wetting layers. The latter are known to give rise to corrections to the Kelvin equation [37,40]. In the $d=2$ Ising model subject to the short-ranged (contact) surface fields one has $H_{ca}(\tau, L) = A(\tau)/L + B(\tau)/L^{4/3}$ to lowest orders in L in the complete-wetting regime [44].

V. NUMERICAL RESULTS AND DISCUSSION

The results of our analysis presented in Ref. [27] (Paper I) assure that the range of temperatures, for which we perform our calculations of the adsorption here, lies above the wetting transition temperature $T_w(p, h_1)$. For $h_1=0.8$ and a short range of the surface fields ($p=\infty$), the wetting temperature in the semi-infinite $d=2$ Ising system equals $T_w(p=\infty, h_1=0.8) \approx 1.41 J/k_B$ and the wetting transition is second order.

Adding the long-ranged tail to the boundary fields shifts the wetting temperature toward lower values.

Using the DMRG method we have carried out calculations of the magnetization profiles $m(j)$ from which we have obtained the thicknesses ℓ_0 of the corresponding wetting layers and the adsorption Γ . The analysis of the shapes of the profiles $m(j)$ and of the scaling properties of ℓ_0 gives a better understanding of the behavior of Γ along different thermodynamic paths. We recall that the predictions for the scaling behavior of the adsorption follows from the scaling behavior of ℓ_0 .

In order to infer possible power laws governing the behavior of the thickness of the wetting layer and of the adsorption along different paths, we have calculated *local exponents* z_i of the quantities of interest as a function of H or τ . They are defined as

$$z_i = \left| \frac{\ln Q(x_{i+1}) - \ln Q(x_i)}{\ln x_{i+1} - \ln x_i} \right|, \quad (15)$$

which is the discrete derivative of data Q as a function of x in a log-log plot; here $Q = \ell_0$ or Γ and $x = H$ or τ . Such a quantity probes the local slope at a given value x_i of x at a point i along the path considered. These local exponents provide a better estimate of the leading exponent than a log-log plot itself. If for large x , Q decays as x^{-z} we have chosen the definition in Eq. (15) such that $z > 0$. The high quality of the DMRG data allows us to reliably carry out the numerical differentiation according to Eq. (15).

A. Isotherms

1. Magnetization profiles

In Figs. 5 and 6 we show a selection of magnetization profiles calculated for a strip width $L=500$ with $p=50$ and 2 along the two isotherms $T^*=1.8$ and $T^*=2.25$ indicated in Fig. 3 as paths (1) and (3), respectively. [We note that there are different scales for j in Figs. 5(a), 5(b), and 6.] From these plots one can see that within the accessible range of values $H < H_{ca}(T, L; p)$, the shapes of the profiles are *not* slablike, even though the system size is very big so that $|H_{ca}(T, L)|$ is expected to be sufficiently small, which allows access to small values of $|H|$ without hitting capillary condensation so that thick wetting films could develop. The profiles are characterized by a pronounced spatial variation at the emerging interface between the spin-up and the spin-down phases, where the profile varies quasilinearly with the distance from the wall, and by extended tails. For the short-ranged case ($p=50$) the profiles along the low-temperature isotherm ($T^*=1.8$) exhibit a rapid decay to their bulk values $m_b \equiv m_b(T, H)$ (< 0 for $H < 0$) with the bulk correlation length $\xi(T, H) = |\tau|^{-\nu} \Xi(H|\tau^\Delta)$ [see Eqs. (6)–(8)] as decay length which increases upon approaching the pseudo-phase-coexistence. Only very close to the pseudo-phase-coexistence line $H_{ca}(T, L; p)$ does the emerging shape of the profile to a certain extent resemble that characteristic of the free interface between the spin-up and the spin-down bulk phases with a broad interfacial region and a rather narrow region where the magnetization stays somewhat close

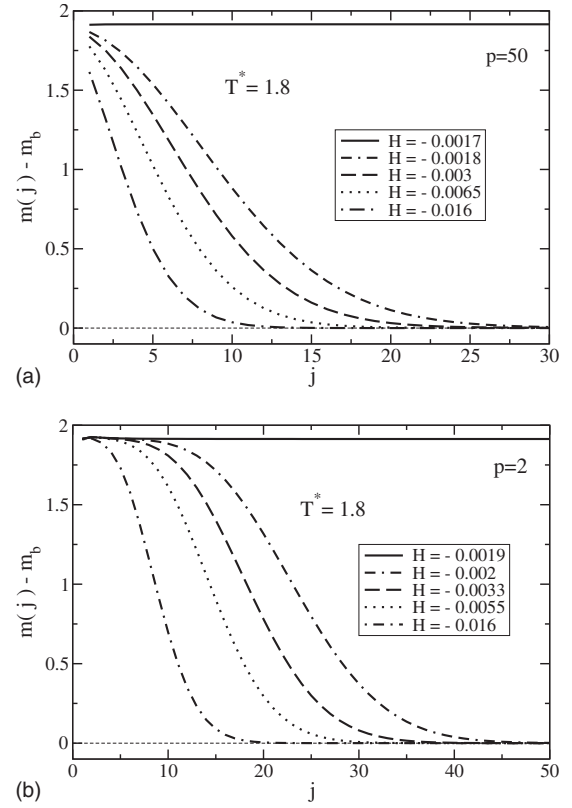


FIG. 5. Magnetization profiles, relative to their bulk values $m_b(T, H) < 0$, near one wall ($j > 1$) along the isotherm $T^* = 1.8$ [see path (1) in Fig. 3], calculated within the DMRG method for $d=2$ Ising strips of width $L=500$, (a) for short-ranged ($p=50$) and (b) for long-ranged ($p=2$) boundary fields of strength $h_1=0.8$. Along this isotherm the pseudo-capillary-condensation transition occurs at $H_{ca} \approx -0.00172$ for $p=50$ and at $H_{ca} \approx -0.00195(4)$ for $p=2$. Thus in (a) and (b) the full lines for $H = -0.0017$ and $H = -0.0019$, respectively, correspond to the capillary filled state with $m(j) - m_b(T, H) \approx 2|m_b(T, H)|$.

to the value $-m_b > 0$ characteristic of the wetting phase corresponding to $H=0^+$. This latter region thickens as $H \rightarrow H_{ca}(T, L; p)$.

For the long-ranged forces ($p=2$) the profiles along the low-temperature isotherm ($T^*=1.8$) exhibit an interfacelike shape already away from the pseudo-phase-coexistence line $H_{ca}(T, L; p)$. The interfacial part of these profiles is much more pronounced than for the short-ranged case ($p=50$) and their decay is much slower. The exponential decay of the profiles to the value $m_b(T, H)$ ultimately crosses over to the power-law decay $\sim j^{-2}$. In general, algebraically decaying interparticle and surface fields are known to generate algebraically decaying order-parameter profiles [45,46].

For both $p=50$ and $p=2$ the profiles corresponding to $H \rightarrow 0$ along the high-temperature isotherm ($T^*=2.25$) decay much slower as compared to the low-temperature isotherm ($T^*=1.8$) and their shapes become different (see Fig. 6). The magnetization in the first few layers near the walls decreases more rapidly so that there the profiles acquire a positive curvature. Further away from the wall there is an inflection point and the narrow plateau occurring near the boundaries for the low-temperature isotherm [see Fig. 5(b)] disappears. The interfacial region becomes very broad.

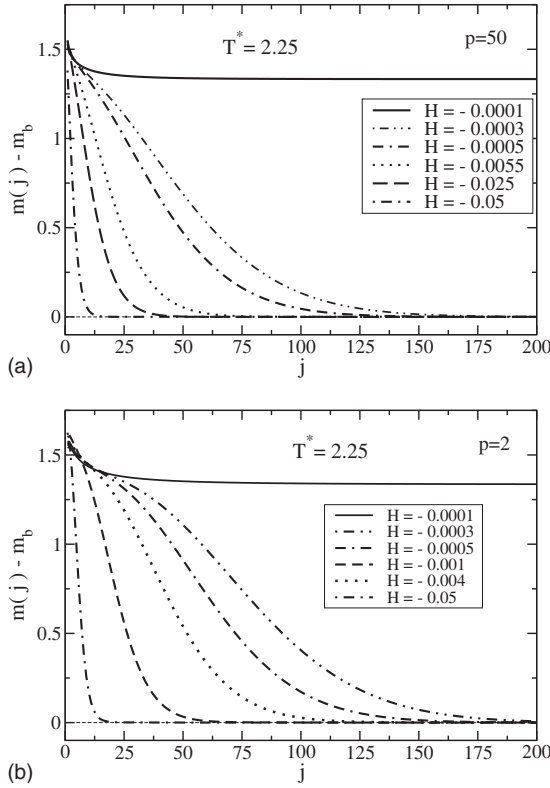


FIG. 6. Magnetization profiles, relative to their bulk values $m_b(T, H) < 0$, near one wall along the isotherm $T^* = 2.25$ [see path (3) in Fig. 3], calculated within the DMRG method for $d=2$ Ising strips of width $L=500$, (a) for short-ranged ($p=50$) and (b) for long-ranged ($p=2$) boundary fields of strength $h_1=0.8$. Along this isotherm the pseudo-capillary-condensation transition occurs at $H_{ca} \approx -0.000191$ for $p=50$ and at $H_{ca} \approx -0.00026(4)$ for $p=2$. Thus in both (a) and (b) the full line for $H=-0.0001$ corresponds to the capillary filled state with $m(j) - m_b(T, H) \approx 2|m_b(T, H)|$.

2. Thickness of the wetting layer

In order to infer thicknesses ℓ_0 of wetting layers from the magnetization profiles, we have chosen the criterion of the change of sign of the curvature of the profile; i.e., we have assigned a thickness of a wetting layer to the profiles which corresponds to the distance $j = \ell_0$ at which the profile exhibits its inflection point. Adopting other criteria for assigning wetting film thicknesses, e.g., the thickness which corresponds to the distance $j = j_0$ at which the magnetization is zero, $m(j_0) = 0$, leads, as it must, to the same conclusions about physical observables.

We have studied the behavior of ℓ_0 along several isotherms. Representative data are shown and discussed below. They correspond to the isotherms $T^* = 1.8$ and $T = T_c$ [see paths (1) and (4), respectively, in Fig. 3] and have been obtained for several strip widths and ranges $p = 50, 5, 4, 3, 2, 1.5$ of the boundary fields. (The data for the isotherms $T^* = 1.6, 1.9, 2, 2.2, \text{ and } 2.25$ are not shown.) We have chosen $h_1 = 0.8$ for which $T_w^*(p=\infty) \approx 1.41$. All considered isotherms lie above the corresponding wetting transition temperatures $T_w(p)$.

Results for the local exponents of $\ell_0(H)$ along the isotherm $T^* = 1.8$ [path (1) in Fig. 3] are shown in Fig. 7. They

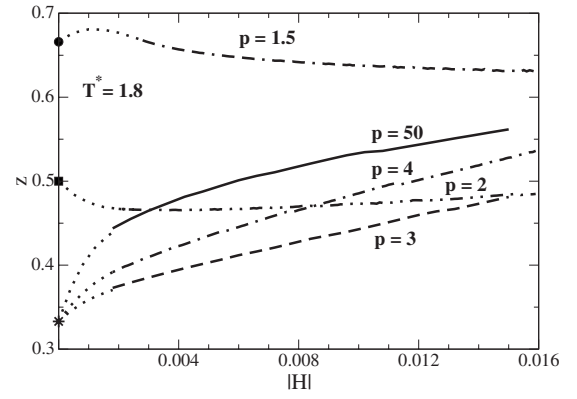


FIG. 7. The local exponents $z(H)$ for $\ell_0(H)$ [see Eq. (15)] calculated along the isotherm $T^* = 1.8$ for $L=500$, $h_1=0.8$, and for the ranges $p=1.5, 2, 3, 4, \text{ and } 50$ of the boundary fields. For $H \rightarrow 0$, without the occurrence of capillary condensation, i.e., for $L \rightarrow \infty$, the expected exponents are $\beta_s^{co} = 1/3$ (\star) for $p=3, 4, \text{ and } 50$, $1/2$ (\blacksquare) for $p=2$, and $2/3$ (\bullet) for $p=1.5$. The values of $H_{ca}(T, L; p)$ are given by the points at which the various lines end on the left. The dotted lines indicate the expected extrapolations $H \rightarrow 0$ for $L \rightarrow \infty$.

were obtained for strips of width $L=500$ with $h_1=0.8$. Path (1) lies entirely within the region between the bulk coexistence curve and the crossover boundary $H_{cr}^{(1)} = -|\tau|^{3\nu}$, with $\nu = 1$ for the $d=2$ Ising model, i.e., within the complete-wetting regime (see Fig. 3). Indeed, for all values of p we observe the increase in ℓ_0 upon approaching the pseudo-phase-coexistence line $H_{ca}(T, L; p)$. The lines in Figs. 7–10 end on the right when they reach the pseudo-phase-coexistence line $H_{ca}(T, L; p)$ (see Fig. 3). Apart from this size dependence of the H window with access for complete wetting, for $L=500$ and 300 (data for $L=300$ are not shown) the finite-size effects are negligible. As expected from the shape of the profiles (see Figs. 5 and 6) for the same value of

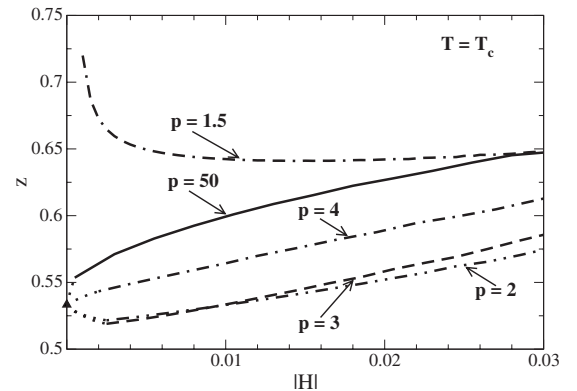


FIG. 8. The local exponents $z(H)$ for $\ell_0(H)$ [see Eq. (15)] calculated along the critical isotherm $T^* = T_c^* = 2.269$ [path (4) in Fig. 3] for $L=500$, $h_1=0.8$, and for the ranges $p=1.5, 2, 3, 4, \text{ and } 50$ of the boundary fields. On the left the curves end at the corresponding capillary condensation point $H_{ca}(T, L; p)$. For $H \rightarrow 0$, without the occurrence of capillary condensation, i.e., for $L \rightarrow \infty$, the expected exponent is $\nu/\Delta = 8/15$ (\blacktriangle). The dotted lines indicate the expected extrapolation for $z(p \geq 2, H \rightarrow 0)$ with $L \rightarrow \infty$. For $p=1.5$ the behaviors of $\ell_0(H)$ and $z(H \rightarrow 0)$ are distinctly different from those for $p \geq 2$.

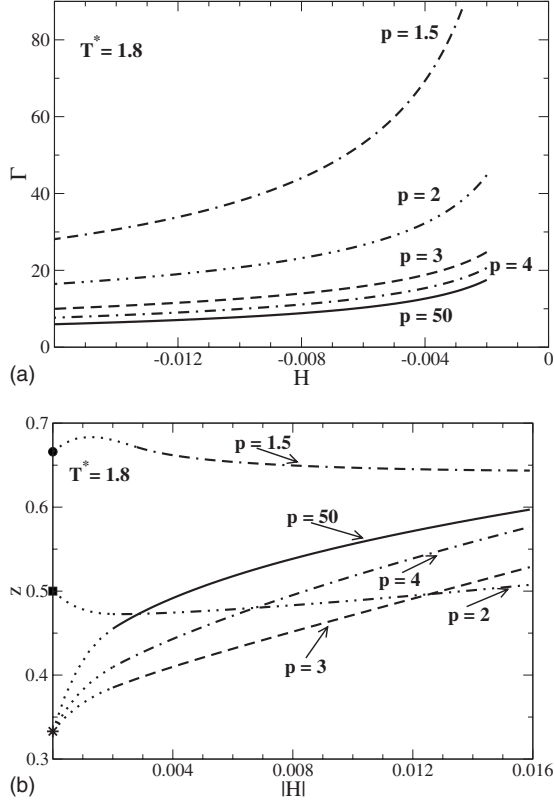


FIG. 9. (a) Adsorption $\Gamma(H)$ and (b) the corresponding local exponents $z(H)$ along the isotherm $T^*=1.8$ [path (1) in Fig. 3] calculated within the DMRG approach for a $d=2$ Ising strip of width $L=500$ subject to symmetric boundary fields of strength $h_1=0.8$ and various ranges p corresponding to power-law decays $\sim j^{-p}$. For small $|H|$ all curves end at $H=H_{ca}(T, L; p)$, where capillary condensation sets in. Dotted lines indicate the expected extrapolations to $H=0$ for semi-infinite systems: $\beta_s^{co}=1/3$ (\star) for $p \geq 3$, $\beta_s^{co}=1/2$ (\blacksquare) for $p=2$, and $\beta_s^{co}=2/3$ (\bullet) for $p=1.5$.

H the wetting layer (data not shown) is much thicker for small values of the exponent p than for short-ranged surface fields ($p=50$).

According to the predictions summarized in Sec. II for semi-infinite systems ($L \rightarrow \infty$), upon approaching the bulk coexistence line $H=0$ the thickness of the wetting film is expected to diverge for $p \geq 3$ with the exponent $\beta_s^{co}=1/3$ and for $p < 3$ with the exponent $\beta_s^{co}=1/p$. As can be inferred from Fig. 7 the local exponents $z(H)$ calculated for $p=50, 40, 3$, and 2 tend toward their predicted values for $H \rightarrow 0$ but cannot reach them due to capillary condensation. The rate of increase in ℓ_0 , as characterized by the behavior of the local exponents $z(H)$, depends on the range of the boundary field p and varies along the isotherm. For $p=1.5$ the local exponents have to behave nonmonotonically in order to reach the expected value $1/p=2/3$. The behavior of ℓ_0 along the isotherm $T^*=1.9$ is very similar (data not shown).

Path (2) corresponds to $T^*=2.0$ and runs in between the crossover lines given by $H_{cr}^{(1)}=-|\tau|^{3\nu}$ and $H_{cr}^{(2)}=-|\tau|^\Delta$, with $\nu=1$ and $\Delta=15/8$ in $d=2$. It hits the pseudo-phase-coexistence line of capillary condensation before it reaches the crossover boundary $H_{cr}^{(1)}=-|\tau|^{3\nu}$. Along that path the variation in ℓ_0 is very similar to the one observed along the iso-

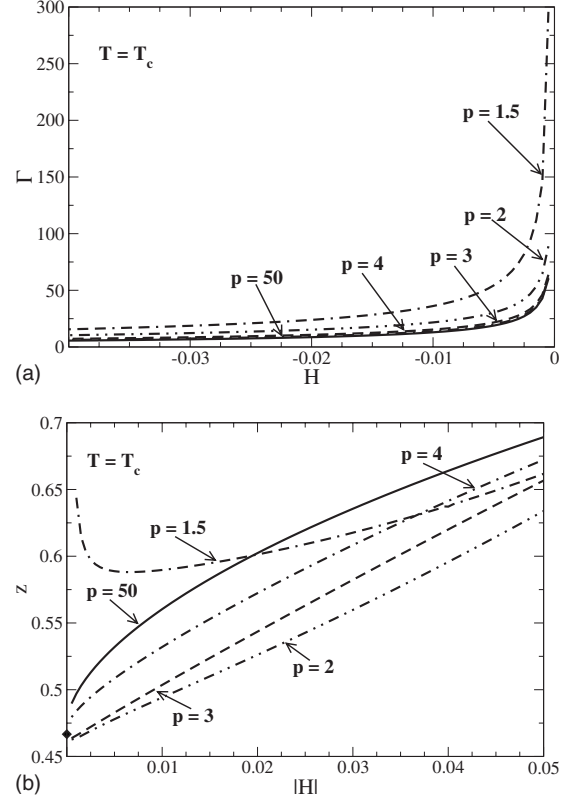


FIG. 10. The same as Fig. 9 along the critical isotherm $T=T_c$ [path (4) in Fig. 3]. In (b) $(\nu-\beta)/\Delta=7/15$ is indicated (\blacklozenge). The crossover to the ultimate complete-wetting behavior is masked by the occurrence of capillary condensation. For $p=1.5$ the behaviors of $\Gamma(H)$ and $z(H \rightarrow 0)$ are distinctly different from those for $p \geq 2$.

therm $T^*=1.8$ with the local exponents approaching the expected values of the complete-wetting regime (data not shown). Again the asymptotic behavior is pre-empted by capillary condensation.

Results along critical ($T^*=T_c^*$) isotherm [path (4) in Fig. 3] are displayed in Fig. 8 for $L=500$. This path lies in the critical-adsorption regime where one expects $\ell_0(H \rightarrow 0) \sim \xi \sim |\Delta H|^{-\nu/\Delta}$, with $\nu/\Delta=8/15$ in $d=2$. This universal behavior is expected to hold if the long-ranged boundary field decays sufficiently rapidly, i.e., if $p > (d+2-\eta)/2$. In this case the long-ranged part of the boundary field is irrelevant in the RG sense with respect to a pure contact surface field [2]. Here η is the critical exponent governing the algebraic decay of the two-point correlation function in the bulk and at T_c . In the present case of the $d=2$ Ising model $\eta(d=2)=1/4$ so that for $p > 15/8$ we expect to observe the power law $\ell_0 \sim |\Delta H|^{-8/15}$.

For $p=1.5$ one has $p < (d+2-\eta)/2$. According to general scaling arguments [2] the magnetization profile for the semi-infinite system under rescaling of distances by a factor of b behave as

$$m_{\pm}(y, \tau, H, h_1, p) = b^{-\beta/\nu} m_{\pm}(yb^{-1}, \tau b^{1/\nu}, Hb^{\Delta/\nu}, h_1 b^{\omega_s}), \quad (16)$$

where $\omega_s \equiv (d+2-\eta)/2-p$. Because in the present case $\omega_s > 0$ the range of such wall-fluid interactions is relevant in the

RG sense at and near T_c ; i.e., the profiles are affected by the decay of the boundary field even if y is sufficiently large. In the critical region the profiles are no longer equivalent to those generated by a pure contact surface field ($p=\infty$). Choosing $b\sim y$ one obtains the scaling form of the magnetization,

$$m_{\pm}(y, \tau, H, h_1, p) = y^{-\beta/\nu} \mathcal{M}_{\pm}(y/\xi_{\tau}, y/\xi_H, y^{\omega_s} h_1), \quad (17)$$

where $\xi_{\tau} \equiv \xi_{\pm}(\tau, 0)$ is given by Eq. (7), whereas $\xi_H \equiv \xi(0, \Delta\mu)$ is given by Eq. (8). For $\omega_s < 0$ and large enough y the scaling functions \mathcal{M}_{\pm} can be expanded in terms of their third argument demonstrating that in this case the long range of the wall-fluid interaction gives rise to contributions to the scaling functions of the magnetization profile which are subleading to the dominant universal $y^{-\beta/\nu}$ behavior valid for $y \leq \xi$ and $p=\infty$. Such an expansion cannot be performed for large y if $\omega_s > 0$. In order to obtain a prediction in this case for the leading behavior of the magnetization profile and hence the thickness of the wetting layer ℓ_0 and the adsorption, one has to calculate the full generalized scaling functions of the magnetization profiles. For $p < 15/8$ such an analysis represents a necessary future research goal which, however, is beyond the scope of the present study. Nevertheless, we find it instructive and stimulating to show our numerical results for $p=1.5$ because they are strikingly different from those obtained for values of p satisfying $p > (d+2-\eta)/2$.

As along the noncritical isotherms $T^* \leq 2.25$ we find that also along the isotherms $T^* = 2.25$ [path (3) in Fig. 3] and $T = T_c^*$ the increase in the wetting film thickness upon approaching $H=0$ is much stronger for $p=1.5$ than for the other values of p (data not shown). Further away from the pseudo-phase-coexistence line, i.e., for $|H| \leq 0.01$ the local exponents attain $z(p=1.5) = 0.64$, which indicates an algebraic increase in ℓ_0 in this range of H with $\ell_0 \approx |H|^{-0.64}$. This effective exponent is close to the value $1/p = 2/3 = 0.66(6)$ predicted for the complete-wetting behavior for $p=1.5$. Closer to $H=0$ the functional form of the increase changes and z increases strongly.

In the limit $H \rightarrow 0$, for $p=50$ and 4 the local exponents seem to approach the expected value of $8/15$ from above, whereas for $p=3$ and 2 they will have to bend upward to do so from below. On the contrary, along the isotherm $T^* = 2.25$ (data not shown) the local exponents for all values of $p > 1.5$ would have to bend upward for $H \rightarrow 0$ in order to reach the expected value of $8/15$.

3. Adsorption

For the present microscopic model in the (symmetric) strip geometry the adsorption Γ is defined as

$$\Gamma = \sum_{j=1}^{L/2} [m_j - m_b(T, H)], \quad (18)$$

where $m_j \equiv \langle \sigma_j \rangle$ is the magnetization in row j and $m_b(T, H)$ is the corresponding bulk magnetization. In the limit $L \rightarrow \infty$ this definition reduces to the semi-infinite quantity Γ defined in Eq. (1). Along the various paths indicated in Fig. 3, at each point we have first calculated the bulk magnetization

$m_b(T, H)$ using an equivalent system but with a vanishing surface field in order to minimize the influence of the boundary. Moreover, for the latter calculations as a representative spin the one in the middle of the strip was taken, as it is the one least affected by finite-size effects. In order to obtain the bulk magnetization $m_b(T, H)$ we have extrapolated this midpoint value $m_{L/2}(T, H; h_1=0)$ to $L \rightarrow \infty$ from data calculated for $L=300, 400, 500, 600,$ and 700 .

The adsorption $\Gamma(H)$ and its local exponents calculated for a strip of width $L=500$ with $h_1=0.8$ and for various ranges p of the boundary fields are shown in Figs. 9 and 10 for paths (1) and (4), respectively, as indicated in Fig. 3. According to the predictions summarized in Sec. II, upon approaching the bulk coexistence line $H=0$ along path (1) ($T^*=1.8$) the adsorption is expected to diverge for $p \geq 3$ with the exponent $\beta_s^{co} = 1/3$. As can be seen in Fig. 9(b) the local exponents calculated for $p=50, 4,$ and 3 tend toward this predicted value for $H \rightarrow 0$ but do not reach it due to the occurrence of capillary condensation.

For $p=2$ the local exponents as a function of the bulk field exhibit a negative curvature, consistent with the behavior of z for the thickness ℓ_0 of the wetting layer (see Sec. V A 2), and seemingly tend to the exponent $1/2$, which agrees with the predicted nonuniversal behavior for $p < 3$, i.e., $\beta_s^{co} = 1/p$. In order to reach the expected exponent $\beta_s^{co} = 2/3$ for $p=1.5$, the local exponents have to vary in a nonmonotonic way for $H \rightarrow 0$ [see Fig. 9(b)]. Path (4) lies in the critical =adsorption regime and one expects [see Eq. (5)] $\Gamma(H \rightarrow 0) \sim |H|^{-(\nu-\beta)/\Delta}$ as $H \rightarrow 0$ for $p \geq 15/8$. One can see from Fig. 10(b) that for both $p=50$ and $p=4$ the local exponents seemingly tend to the predicted value $(\nu-\beta)/\Delta = 7/15$ from above. In order to reach this value for $p=3$ and 2, the local exponents have to bend upward for $H \rightarrow 0$. The same holds along the isotherm $T^* = 2.25$ [data for path (3) not shown], but whether the local exponents ultimately tend to the complete-wetting values $\beta_s^{co} = 1/3$ and $1/2$, respectively, after crossing both crossover lines $H_{cr}^{(1)}$ and $H_{cr}^{(2)}$ is unclear because for the finite values of L considered here the asymptotic behavior is pre-empted by capillary condensation. (Note that for $\beta_s^{co} = 1/2$ one has $H_{cr}^{(1)} = |\tau|^{2\nu}$.) According to Fig. 3 for $T^* = 2.25$ this complete-wetting regime is expected to be very narrow. For $p=1.5$ ($< 15/8$) the behavior of the critical adsorption is expected to be nonuniversal. Indeed, as compared to the other values of p we observe a distinctly different behavior of the local exponents along path (4) with $z(H \rightarrow 0)$ strongly increasing. (Note that for $p=1.5$ one has $H_{cr}^{(1)} = |\tau|^{3\nu/2}$.)

Due to the scaling behavior $H_{ca}(\tau, L) \sim |\tau|^{\Delta-\nu}/L$, for $L \gg 1$ but fixed, the pseudo-capillary-condensation line appears to approach the bulk critical point (but without reaching it actually due to $L < \infty$) as $|\tau|^{\Delta-\nu} = |\tau|^{7/8}$, which is a weaker power law than $|H_{cr}^{(1)}| \sim |\tau|^{\nu/\beta_s^{co}} = |\tau|^3$ for the crossover line to complete wetting. This explains the observation that in $d=2$, upon approaching bulk coexistence sufficiently close to the critical point, the asymptotic complete-wetting regime is always pre-empted by capillary condensation. More generally, we expect that in *confined* systems the asymptotic complete-wetting divergence of the adsorption can be observed only if $\Delta - \nu = 2 - \alpha - \beta - \nu > \nu/\beta_s^{co}$. This condition is

fulfilled neither in $d=2$ with $\Delta-\nu=0.875$ and $\nu/\beta_s^{co}=3$ nor in $d=3$ with $\Delta-\nu=0.936$ and $\nu/\beta_s^{co}=3\nu=1.89$. Thus we conclude that along an isotherm close to T_c the ultimate crossover to the complete-wetting behavior can only be observed in systems with macroscopically large transverse extensions.

B. Thermodynamic path along the pseudo-phase-coexistence line

In the present confined system the analog of the thermodynamic path parallel to the bulk coexistence line on the gas side with a small undersaturation $\Delta\mu=\text{const}>0$ and with $T\rightarrow T_c$ is the thermodynamic path $H_{(0)}(T,L)=H_{ca}(T,L)+\delta H$ along the pseudo-phase-coexistence (capillary condensation) line $H_{ca}(T,L)$ shifted slightly by δH to the spin-down ($\sigma=-1$) side [see path (0) in Fig. 3]. In view of the large computational effort required for the determination of the curve $H_{ca}(T,L)$ and of the value of the bulk magnetization $m_b(T,H)$, at each point along this line we have calculated the adsorption along this path only for a short-ranged boundary field ($p=50$), for the $p=3$ of long-ranged surface fields, and for $p=2$. We have considered three constant shifts away from the pseudo-phase-coexistence line: $\delta H=-10^{-5}$, -10^{-6} , and -10^{-7} .

1. Magnetization profiles

In Fig. 11 we have plotted a selection of magnetization profiles $m(j)$ along the thermodynamic path shifted by a constant -10^{-6} away from the pseudocoexistence line $H_{ca}(T,L)$ for $p=50$ [Fig. 11(a)] and for $p=2$ [Fig. 11(b)]. For $p=3$ the profiles look qualitatively the same as for $p=2$; they are both characterized by a much broader interfacial region and larger tails than the ones for $p=50$. The shape of the profiles changes upon approaching bulk coexistence $H=0$ in a way similar to the case along the near-critical isotherm $T^*=2.25$. One observes a broadening of the interfacial region together with a rather small region where the magnetization stays close to the value $m_b(T,H)>0$ characteristic of being slightly on the upper side of the bulk coexistence curve, i.e., $H=0^+$.

2. Thickness of the wetting layer

For three undersaturations δH relative to the pseudo-phase-coexistence line Fig. 12(a) shows the thickness of the wetting layers as a function of temperature calculated for a fixed strip width $L=340$ with strength $h_1=0.8$ and ranges $p=50, 3, 2$ of the boundary fields. The increase in the thickness of the wetting layer along these paths is very similar for all considered values of the decay exponent p .

At low temperatures, for $p=2$ the wetting layer is about three times thicker than for the short-ranged boundary field. Except for the close vicinity of the critical temperature, i.e., for $-0.98\leq T^*-T_c^*\leq 1.01$, where the finite-size effects are very pronounced, results obtained along paths with different shifts δH but the same p collapse onto a common curve. We note that for $p=50$ this common curve splits into three different lines just above the pseudocritical temperature $T_{c,L}^*(L=340, h_1=0.8)\approx 2.2$, i.e., where the pseudocoexistence line $H_{ca}(T,L)$ intersects the crossover line $H_{cr}^{(2)}=-|\tau|^\Delta$. For each p

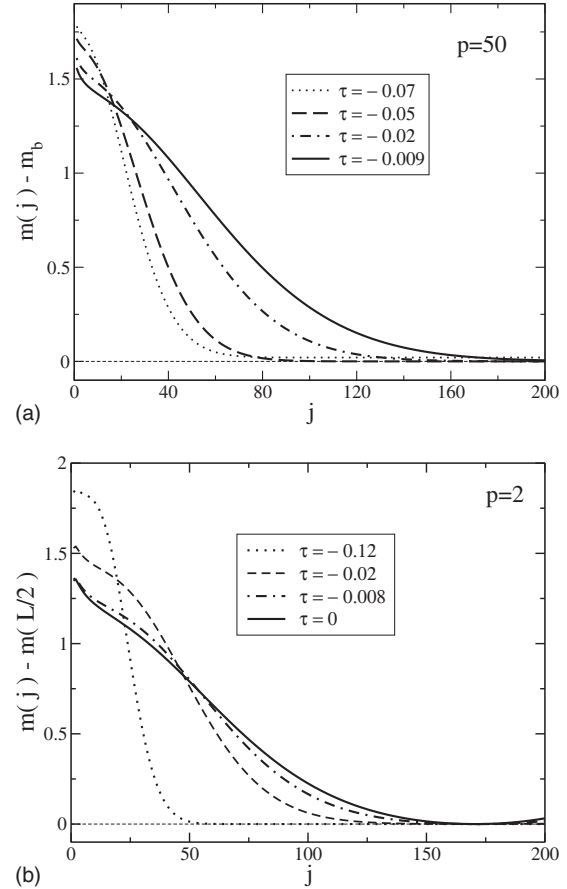


FIG. 11. Magnetization profiles near a single wall, relative to their bulk values $m_b(T,H)$, along thermodynamic path (0) (see Fig. 3) shifted by a constant of -10^{-6} away from the pseudo-phase-coexistence line $H_{ca}(T,L)$, calculated within the DMRG method for $d=2$ Ising strips of width $L=700$ for short-ranged [(a) $p=50$] and of width $L=340$ for long-ranged [(b) $p=2$] boundary fields of strength $h_1=0.8$. Due to the slow decay, the profiles for $p=2$ are presented relative to their values $m(L/2) \neq m_b(T,H)$ at the midpoint of the film.

the thickness of the wetting film attains a certain L -dependent value at the bulk critical temperature T_c , which also depends on the value δH of the shift of path (0). In order to calculate $\ell_0(T=T_c)$ for large L we have performed an extrapolation scheme for the curves $\ell_0(T)$ to $T=T_c$, not taking into account data for temperatures higher than $T^*=2.24$ because those exhibit pronounced finite-size effects beyond the leading L behavior. For $p=50$ we have found (data not shown) that the thickness of the wetting layer at $T=T_c$ is proportional to L , which is expected because ℓ_0 cannot grow larger than $L/2$. For $p\geq 2$ it should diverge for $L\rightarrow\infty$. Above T_c we observe a rapid decrease in ℓ_0 as function of T .

For increasing $T\leq T_c$ in Fig. 12(a) we observe a continuous increase in the thickness of the wetting layer. We recall that, according to effective interface Hamiltonian studies, sufficiently far away from criticality, i.e., for $\ell_0\gg\xi$, the wetting layer thickness should be independent of temperature along the path of constant undersaturation $\Delta\mu$, i.e., $H=\text{const}$ with respect to bulk coexistence (see the last paragraph of Sec. II). The present results are calculated along

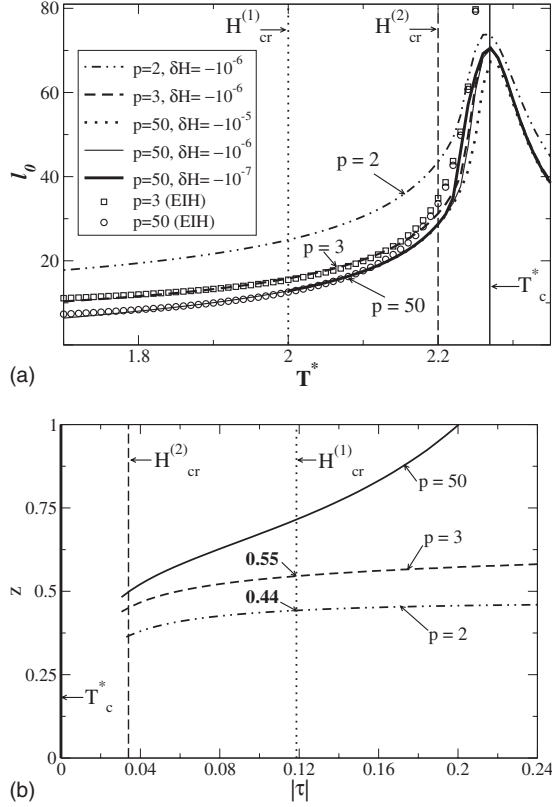


FIG. 12. (a) Wetting layer thickness ℓ_0 (defined as in Fig. 8) as a function of temperature T^* calculated for $L=340$, $h_1=0.8$, and various values of the exponent p , characterizing the range of the boundary fields, along path (0) in Fig. 3 with constant shift $\delta H=-10^{-6}$ away from the pseudo-phase-coexistence line $H_{ca}(T,L;p)$ (see main text). For $p=50$, in addition the temperature dependence of ℓ_0 for shifts $\delta H=-10^{-5}$ and -10^{-7} is shown (dotted and thick solid lines, respectively). Symbols denote predictions from the effective interface Hamiltonian (EIH) for $p=50$ (circle) and for $p=3$ (square) (see main text). (b) The local exponents $z(\tau)$ for ℓ_0 calculated from the data with constant shift $\delta H=-10^{-6}$ shown in (a) as a function of $\tau=(T-T_c)/T_c$. At the dotted and dashed vertical lines the thermodynamic paths pass through the crossover lines $H_{cr}^{(1)}$ and $H_{cr}^{(2)}$, respectively, shown in Fig. 3 (and *de facto* independent of δH). Due to the finite peak of ℓ_0 at T_c , below $H_{cr}^{(2)}$, i.e., for $|\tau| \leq 0.04$, the concept of the local exponents turns out to be less useful so that the lines in (b) have not been continued into this region.

$H=H_{(0)}(L,T)=H_{ca}(T,L)+\delta H$ with $\delta H=\text{const}<0$ such that $|H|$ decreases for increasing temperatures, which should result in thicker films. This is in accordance with the data in Fig. 12(a). In order to check whether this increase is captured by effective interfacial models we adopt a simple, renormalized effective interface potential $\bar{W}(\ell)$ valid for quasi-short-ranged ($p=50$) boundary fields as well as for long-ranged boundary fields with a decay exponent $p=4$ or 3. Taking an undersaturation H into account, we make the ansatz [3] (in units of $k_B T_c / a^2$)

$$\bar{W}(\ell) = \bar{A}\ell^{-(p-1)} + B\ell^{-\kappa} + (|H|\Delta m)\ell, \quad (19)$$

where an effective repulsive interaction $\sim B$, which accounts for the gain in entropy of the unbinding interface, has to be

added to the leading long-ranged potential energy term $\sim \bar{A} > 0$ (see Sec. II A) [31]. One has $B=B_0 k_B T / \Sigma(T) > 0$ [31], where $\Sigma(T)$ is the surface stiffness of the interface, $B_0 = \text{const}$, and $\Delta m = 2|m_b^{(0)}(T)|$. The exponent κ describing thermal wandering is given by $\kappa = 2(d-1)/(3-d)$, which equals 2 in $d=2$ (see Sec. II A) [31]. $\bar{W}(\ell)$ is thought of to emerge from renormalization of the bare effective interface potential $W(\ell)$ (see Eq. (1) of our preceding work [27]) due to the fluctuations of the depinning interface.

In Eq. (19) the second (entropic) term dominates in $d=2$ for $p > 3$. Thus for short-ranged forces ($p \gg 1$) the equilibrium wetting film thickness varies as function of T along a thermodynamic path $H(T)$ as

$$\ell_0 = \{B_0 k_B T / [\Sigma(T) |m_b^{(0)}(T)|]\}^{1/3} |H(T)|^{-1/3}, \quad p > 3. \quad (20)$$

For $p=3$ the entropic term competes with the interaction term. This leads to the equilibrium thickness of the wetting film,

$$\ell_0 = \{[\bar{A} + B_0 k_B T / \Sigma(T)] / |m_b^{(0)}(T)|\}^{1/3} |H(T)|^{-1/3}, \quad p = 3. \quad (21)$$

\bar{A} is proportional to $\Delta m = 2|m_b^{(0)}(T)|$ so that $\bar{A}/|m_b^{(0)}(T)|$ only weakly depends on T . For $p < 3$ the first term in Eq. (19) dominates and the temperature dependence of the film thickness follows that of $H(T) \approx H_{ca}(T,L)$, if the system is moved thermodynamically along the pseudocoexistence line $H_{ca}(T,L)$:

$$\ell_0 = \left[\frac{p-1}{2} \frac{\bar{A}}{|m_b^{(0)}(T)|} \right]^{1/p} |H_{ca}(T,L)|^{-1/p}, \quad p < 3. \quad (22)$$

For the $d=2$ Ising model the surface stiffness is known exactly [47] as $\Sigma(T)/(k_B T) = \sinh[2(K-K^*)]$, where $K = J/(k_B T)$, $K-K^* \approx -2K_c \tau$. Both $\Sigma(T)$ and $\Delta m(T) \equiv 2|m_b^{(0)}(T)|$ decrease with increasing temperature. Therefore, for all values of p , ℓ_0 is expected to increase along the pseudocoexistence line $H_{ca}(T,L)$.

We note that with $\bar{A} > 0$ the ansatz in Eq. (19) is arranged such that at sufficiently high temperatures (i.e., above the wetting transition temperature) $\bar{W}(\ell)$ renders complete wetting for $p < 3$. The occurrence of complete wetting for $p < 3$ is supported by the numerical results for the full microscopic model obtained in Ref. [27], which are, however, at variance with the predictions of a simple effective interface model based on the bare potential $W(\ell) = -A\ell^{-(p-1)}$ with $A > 0$ [see Eq. (2) of Ref. [27]].

Sufficiently close to the bulk critical point the surface stiffness vanishes with the same power law as the surface tension of the interface σ , i.e., $\Sigma(\tau \rightarrow 0) \sim \sigma \sim |\tau|^{(d-1)\nu} = |\tau|$ for the $d=2$ Ising model. Since $\Delta m \sim |\tau|^\beta$ it follows that in the critical region for short-ranged forces

$$\begin{aligned} \ell_0 &\sim |\tau|^{-[\beta+(d-1)\nu]/3} |H_{ca}(\tau,L)|^{-1/3} \\ &= |\tau|^{-3/8} |H_{ca}(\tau,L)|^{-1/3}, \quad p = 3. \end{aligned} \quad (23)$$

with $H_{ca}(\tau,L)$ given by Eq. (14).

Close to T_c and in the temperature range for which the pseudocoexistence line $H_{ca}(\tau, L)$ lies in between the crossover lines $H_{cr}^{(1)} = -|\tau|^{3\nu}$ and $H_{cr}^{(2)} = -|\tau|^\Delta$, we have found (see Fig. 4), for both $p=50$ and $p=3$, that the absolute value of the scaling function $\hat{g}(x=L/\xi)$ of the pseudocoexistence line [see Eq. (14)] decreases and crosses over from the power-law behavior $\hat{g}(x \rightarrow \infty) \sim x^w$, with $w \approx 0.75$ for $|\tau| \neq 0$, to a constant value $\hat{g}(x=0)$ at $\tau=0$. This implies that for decreasing $|\tau|$, $\ell_0(\tau)$ crosses over from an increase of $\sim |\tau|^{-5/8}$ to one of $\sim |\tau|^{-3/8}$ (for L fixed). Thus the effective interface model predicts that along path (0), $\ell_0(\tau \rightarrow 0)$ is an increasing function of temperature. But in view of the aforementioned crossover one cannot expect a purely algebraic behavior in this region.

For $12 \leq L|\tau|^\nu \leq 50$, the variation in the pseudocoexistence line $H_{ca}(T, L)$ at fixed L is approximately algebraic with an effective exponent $w \approx 0.75$. Inserting $H = H_{ca}(T, L) \sim |\tau|^{0.75}$ into the expression for ℓ_0 [Eq. (23)] gives $\ell_0 \sim |\tau|^{-0.625}$ for both $p=50$ and $p=3$. For $L|\tau|^\nu \ll 1$ one has $H_{ca} \rightarrow \text{const}$, so that in this limit Eq. (23) predicts $\ell_0(\tau \rightarrow 0) \sim |\tau|^{-3/8}$.

For $p=2$ the pseudocoexistence line $H_{ca}(T, L)$ seems to follow a power law with the same effective exponent as for $p=50$ and 3 for reduced temperatures smaller than the crossover line $H_{cr}(1)$ (see Fig. 3). Therefore on the basis of Eq. (22) for $12 \leq L|\tau|^\nu \leq 50$ one expects $\ell_0 \sim |\tau|^{-0.375}$.

For $p=50$ the behavior of the local exponents $z(\tau)$ determined from the numerical data obtained for $L=340$ and shown in Fig. 12(a) is consistent with the above predictions [see Fig. 12(b)]. We find that in between the crossover lines $H_{cr}^{(1)} = -|\tau|^{3\nu}$ and $H_{cr}^{(2)} = -d_2|\tau|^\Delta$ the local exponents z decrease continuously upon decreasing $|\tau|$. For $0.12 \leq L|\tau|^\nu \leq 50$, which with $L=340$ and $\nu=1$ corresponds to $0.04 \leq |\tau| \leq 0.15$, the value of z for $p=50$ changes from ≈ 0.80 to ≈ 0.52 . No saturation at the value of 0.625, which would reflect the power law $\hat{g}(x) \sim x^{0.75}$ [see Eq. (14) and the discussion above], is observed. However, the above temperature range lies outside the range of validity of the asymptotic power-law behaviors of $\Sigma(T)$ and $\Delta m(T)$, leading to deviations from the algebraic variation $\ell_0 \sim |\tau|^{-0.625}$ discussed above.

In order to test the validity of the effective interface Hamiltonian approach, we compare our full DMRG data with the predictions for the increase in the wetting film thickness along the line of pseudo-phase-coexistence $H_{ca}(T, L)$ stemming from Eq. (20) by inserting our numerical data for $H(T) = H_{ca}(T, L)$ and $\Delta m(T) = 2|m_b(T)|$ and by using the analytic expression for $\Sigma/(k_B T)$ given above. Treating B_0 as a fitting parameter we find very good agreement between these two approaches for $B_0 = 0.729$ [see Fig. 12(a)] in a wide temperature range below $T^* \approx 2.215$. We note that for higher temperatures the system crosses over to the critical-adsorption regime (beyond the crossover line $H_{cr}^{(2)}$).

For $p=3$ and 2 we observe that at $H_{cr}^{(1)}$ the local exponents z saturate at the values ≈ 0.55 and ≈ 0.44 , respectively. In the case $p=3$ the exponent is slightly smaller than the prediction of 0.625 based on the scaling behavior obtained within the effective interface model, whereas for $p=2$ it is slightly larger than the value of 0.375 expected also within the effective interface model.

We repeat the procedure described above to check the agreement of the effective interface Hamiltonian prediction

in Eq. (21) with our DMRG data for $p=3$. We adopt $B_0 = 0.729$, i.e., the value determined from the fitting of Eq. (20) to the DMRG results for $p=50$, and treat $\bar{A}/|m_b(T)| \approx \text{const} \equiv C$ as a free parameter. Very good agreement is obtained for $C \approx 1.5$ and temperatures $T^* \leq 2.15$ [see Fig. 12(a)].

However, the assumption $\bar{A}/|m_b(T)| \approx \text{const}$ does not lead to agreement of the DMRG data for $p=2$ (not shown) with the curve predicted by Eq. (22) with $H(T) = H_{ca}(T, L)$. Thus we conclude that in the case $p=2$ (not shown) the simple effective interface Hamiltonian given by Eq. (19) fails to describe the full DMRG data. This matches with the conclusions drawn in Ref. [27], where it was found that for $p < 3$ a simple effective interface Hamiltonian wrongly predicts the absence of continuous wetting transitions for these long-ranged substrate potentials.

3. Adsorption

Results for the adsorption obtained for $L=340$, $h_1=0.8$, and $p=50, 3, 2$ are shown as a function of T in Fig. 13(a).

In accordance with the expectations, the behavior of $\Gamma(T)$ upon increasing the temperature is qualitatively similar to the behavior of $\ell_0(T)$ in Fig. 12(a).

According to the discussion in the last paragraph of Sec. II, for $p \geq 3$ and in between the two crossover lines $H_{cr}^{(1)} = -|\tau|^{3\nu}$ and $H_{cr}^{(2)} = -|\tau|^\Delta$ (see Fig. 3), Γ is expected to increase $\sim |\tau|^{-(\nu-\beta)}$, which for $d=2$ corresponds to an exponent of -0.875 , provided the variation in ξ is dominated by its dependence on τ [Eq. (7)]. This is the case along paths of constant undersaturation $\Delta\mu \equiv H = \text{const}$. Along the pseudocoexistence line and for $p=50$ the local exponents of Γ vary strongly with temperature, also below the crossover line $H_{cr}^{(1)}$ [see Fig. 13(b)]. This is not compatible with the aforementioned algebraic variation in Γ for $H = \text{const}$. In view of the discussion of the corresponding behavior of the wetting film thickness in Sec. V B 2, this difference can be traced back to the fact that the pseudocoexistence line does not run parallel to the bulk coexistence line. Due to $\Gamma \sim \ell_0 \Delta m$ and the fact that Δm decreases upon decreasing the reduced temperature $|\tau|$, one expects that the increase in Γ is weaker than the increase in ℓ_0 . This is consistent with our numerical data for the local exponents $z(\tau)$. At each point along path (0) the value of $z(\tau)$ obtained for Γ is smaller than the corresponding value of z obtained for ℓ_0 [see Figs. 12(b) and 13(b)].

For $p=3$ and $p=2$ the variation in the local exponents of the adsorption in the temperature range in between the crossover lines $H_{cr}^{(1)}$ and $H_{cr}^{(2)}$ is less pronounced than that for $p=50$. Near $H_{cr}^{(1)}$ we find saturation for the local exponents $z(\tau)$ at values which are smaller than the saturation values of $z(\tau)$ of the corresponding thickness ℓ_0 of the wetting film, i.e., $z \approx 0.49$ and $z \approx 0.36$ for $p=3$ and $p=2$, respectively [see Fig. 13(b)]. This is consistent with the relation $\Gamma \sim \ell_0 \Delta m$ and can be explained by the same arguments as used in Sec. V B 2. We note that $\Delta m \sim |\tau|^\beta$, with $\beta = 1/8 = 0.125$ for the $d=2$ Ising model, leads to bigger differences in the local exponents for ℓ_0 and Γ than the aforementioned ones observed in the range of their saturation [$p=3$: $z(\ell_0) - z(\Gamma) = 0.55 - 0.49 = 0.06 < 0.125$; $p=2$: $z(\ell_0) - z(\Gamma) = 0.44 - 0.36 = 0.08 < 0.125$].

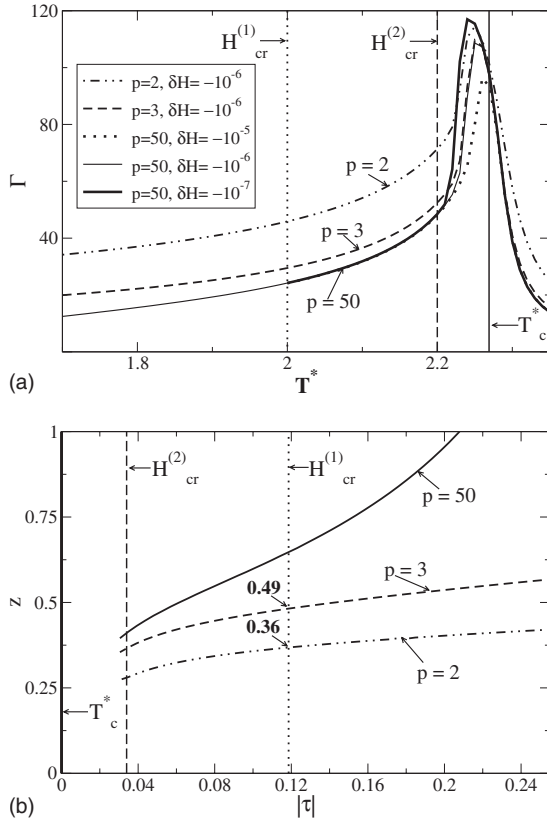


FIG. 13. (a) Adsorption Γ as a function of T^* along path (0) in Fig. 3 with a constant shift $\delta H=-10^{-6}$ away from the pseudo-phase-coexistence line $H_{ca}(T,L;p)$ (see main text), calculated within the DMRG method for $d=2$ Ising strips of width $L=340$ for short-ranged ($p=50$) and long-ranged ($p=3,2$) boundary fields of strength $h_1=0.8$. For $p=50$ the temperature dependence of Γ is also shown for shifts $\delta H=-10^{-5}$ and -10^{-7} (dotted and thick solid line, respectively). (b) The local exponents $z(\tau)$ for Γ calculated from the data shown in (a) for the constant shift $\delta H=-10^{-6}$. At the dotted and dashed vertical lines the thermodynamic path passes through the crossover lines $H_{cr}^{(1)}$ and $H_{cr}^{(2)}$, respectively, shown in Fig. 3 (and *de facto* independent of δH). As in Fig. 12(b), in (b) the lines do not continue into the region $|\tau| \leq 0.04$.

However, the above power laws are satisfied only sufficiently close to T_c , which is not reached along $H_{ca}(T,L)$ for the finite values of L studied here.

VI. SUMMARY AND CONCLUSIONS

We have studied two-dimensional Ising ferromagnets in strip geometries of width L and with long-ranged boundary fields ($V_j^s = \frac{h_1}{j^p}$, $h_1 > 0$) [Eqs. (9) and (10)]. Based on scaling theory and the density-matrix renormalization-group method we have obtained the following main results:

(1) In Secs. I and II we have discussed the theoretical framework and the expectations due to scaling theory for the interplay between critical adsorption and complete wetting, including the crossover between them. For semi-infinite systems the corresponding scaling arguments lead to the schematic phase diagram shown in Fig. 1.

(2) The location of the pseudo-phase-coexistence line $H_{ca}(T,L;p)$ of capillary condensation has been determined for various ranges p of the boundary fields (Fig. 3). For positive and parallel surface fields capillary condensation occurs at negative values $H_{ca}(T,L;p)$ of the bulk field H . Increasing the range of the boundary fields shifts the pseudo-phase-coexistence line toward more negative values of the bulk field H (see Fig. 3). Relative to the pseudo-capillary-condensation line, in the case that the surface fields act only on the two boundary layers $j=1$ and $j=L$, i.e., for $p=\infty$, $H_{ca}(T,L;p)$ varies exponentially as function of the range p .

(3) The finite-size scaling predictions for the capillary condensation line [see Eqs. (13) and (14) as well as Figs. 2 and 4] are satisfied for both short-ranged ($p=50$) and long-ranged ($p=3$) boundary fields.

(4) Within the accessible range of values for T and H , the shapes of the magnetization profiles both along isotherms (see Figs. 5 and 6) and along the pseudo-capillary-condensation line (see Fig. 3) are not slablike. They exhibit a wide interfacial region and significant tails. Primarily the profiles approach their plateau values in the middle of the strip exponentially as function of the distance from the wall. The width of the emerging interfacial region and the decay length of the tails are proportional to the bulk correlation length and thus grow upon approaching T_c or the pseudo-capillary-condensation line. In the presence of long-ranged boundary fields the exponential decay of the profiles toward their bulk values $m_b(H,T)$ is followed by an algebraic decay j^{-p} which finally is distorted by the presence of the distant wall. Features similar to those of these order-parameter profiles have been inferred from neutron reflectometry for the composition profile of a wetting film in a binary-liquid mixture of *n*-hexane and perfluoro-*n*-hexane [48].

(5) The variation in the thickness ℓ_0 of the wetting layer along various isotherms (Figs. 7 and 8) and along the pseudo-phase-coexistence line (Fig. 12) has been analyzed for wide strips and different ranges p of the boundary field. Along both types of path we have found a gradual increase in ℓ_0 upon approaching T_c . The asymptotic divergence of ℓ_0 along the isotherms is pre-empted by capillary condensation. As discussed on general grounds at the end of Sec. V A 3, in both $d=2$ and $d=3$ along the isotherm close to T_c the ultimate crossover to the complete-wetting behavior [see hatched region and path (II) in Fig. 1] can only be observed in systems with macroscopically large transverse extensions. Along the isotherms and within the complete-wetting regime the suitably defined local exponents of ℓ_0 [Eq. (15)] tend to approach the values predicted by the corresponding effective interface Hamiltonian, i.e., $\beta_s^{co}=1/3$ for $p \geq 3$ and $\beta_s^{co}=1/p$ for $p < 3$ (Fig. 7). These results show that there is a complete-wetting regime also for the values $p=2$ and 1.5 of the decay exponent of the boundary field, i.e., smaller than the marginal case $p=3$. This is consistent with the findings in Ref. [27] which demonstrate the existence of a critical wetting transitions for these values of p . Along the pseudo-phase-coexistence line $H_{ca}(T,L)$ the variation in the thickness of the wetting film is determined by the functional form of the temperature dependence of $H_{ca}(T,L)$ and for $p > 3$ it agrees with the predictions of an effective interface Hamiltonian [Eq. (20) and Fig. 12(a)]. This is compatible with the

findings of Ref. [27], in which the use of effective interface Hamiltonians is questioned for $p \leq 3$. For long-ranged boundary fields with $p=3$ and $p=2$, the increase in ℓ_0 within a certain range of temperature can be described by a power law with an effective exponent which is, however, not universal. It varies from approximately 0.55 for $p=3$ to approximately 0.44 for $p=2$ [Fig. 12(b)].

(6) For $p=50, 4, 3$, and 2 the adsorption Γ [Eqs. (1) and (18)] has been calculated along various isotherms (see Figs. 9 and 10). Along these thermodynamic paths, over a wide range of the bulk field H the adsorption Γ exhibits a continuous increase upon approaching the pseudo-phase-coexistence line $H_{ca}(T, L; p)$. Within the accessible range of values for H this increase cannot be described by simple power laws. Only very close to $H_{ca}(T, L; p)$ do the local exponents of Γ start to approach their predicted values, i.e., $\beta_s^{co}(p \geq 3) = 1/3$ and $\beta_s^{co}(p=2) = 1/2$ for complete wetting (see Sec. II A and Fig. 9) and $(\nu - \beta)/\Delta = 7/15$ for critical adsorption [see Eq. (5), Sec. II B, and Fig. 10]. However, these results are not entirely conclusive because the asymptotic regimes are pre-empted by capillary condensation so that one is unable to detect the crossover from critical adsorption to complete wetting which is expected to occur sufficiently close to bulk coexistence for isotherms with T close to T_c . For the low-temperature isotherms, which lie entirely within the complete-wetting regime, the cases $p=1.5, 2$, i.e., for p smaller than the marginal value $p=3$, differ distinctly from the cases $p \geq 3$ (see Sec. II A and Fig. 9), which is a clear indication of the nonuniversality of complete wetting for these cases. For $p=1.5$ the long-ranged part of the boundary field is relevant in the RG sense and the behavior of Γ is nonuniversal along the critical isotherm [see Fig. 10(b)].

(7) For $p=50, 3$, and 2 the magnetization profiles (Fig. 11) and the adsorption Γ (Fig. 13) have been calculated along the pseudo-capillary-condensation line $H_{ca}(T, L)$. Over a wide range of temperatures below T_c , Γ increases gradually (see Fig. 13). Near criticality its increase cannot, however, be described by a simple power-law behavior. The reason is that

along this thermodynamic path the temperature dependence of Γ is determined also by the temperature variation in $H_{ca}(T, L)$, similarly as with the thickness ℓ_0 of the wetting film, which is approximately related to Γ as $\Gamma \approx \ell_0 \Delta m$, where $\Delta m(T)$ is the temperature-dependent difference between the magnetization of the spin-up and the spin-down bulk phases. Our theoretical results cannot be directly compared with the experimental findings in Refs. [12,13], in which the thickness of the wetting layer [12] and the adsorption [13] were measured along the paths corresponding to path (1) in Fig. 1; i.e., in these experiments the capillary condensation was absent. The data obtained from both experiments show that the behavior of ℓ_0 and Γ can be described by a power law but with an effective exponent which differs from both that for complete wetting and that for critical adsorption. Similarly, in our theoretical analysis of two-dimensional Ising strips, for long-ranged boundary fields with $p=3$ and $p=2$ the increase in Γ , for still sufficiently large reduced temperatures $|\tau|$, can be described by a power law with an effective exponent, here with a value of approximately 0.44 for $p=3$ and of approximately 0.36 for $p=2$ (Fig. 13).

(8) Our results indicate that the asymptotic behavior for $H \rightarrow 0$ occurs in a much narrower regime than one would expect and therefore requires much larger system sizes to suppress capillary condensation sufficiently in order to reach the asymptotic regime. One indication for having entered the asymptotic regime could be that a fully developed wetting layer has been formed. For the system sizes L and thus the values of H accessible in our calculations this does not yet fully occur.

ACKNOWLEDGMENTS

A.D. thanks the Wrocław Centre for Networking and Computing (Grant No. 82) and the Computing Center of the Institute of Low Temperature and Structure Research PAS for access to their computing facilities. A.M. and A.D. acknowledge discussions with R. Evans.

-
- [1] K. Binder, in *Phase Transitions and Critical Phenomena*, edited by C. Domb and J. L. Lebowitz (Academic, London, 1983), Vol. 8, p. 1.
- [2] H. W. Diehl, in *Phase Transitions and Critical Phenomena*, edited by C. Domb and J. L. Lebowitz (Academic, London, 1986), Vol. 10, p. 76.
- [3] S. Dietrich, in *Phase Transitions and Critical Phenomena*, edited by C. Domb and J. L. Lebowitz (Academic, London, 1988), Vol. 12, p. 1.
- [4] Y. Xia, B. Gates, Y. Yin, and Y. Lu, *Adv. Mater. (Weinheim, Ger.)* **12**, 693 (2000).
- [5] E. Bertrand, *J. Pet. Sci. Eng.* **33**, 217 (2002).
- [6] P. G. de Gennes, *Rev. Mod. Phys.* **57**, 827 (1985).
- [7] P. Tabeling, *Microfluidics* (EDP Sciences, Paris, 2004).
- [8] *Supercritical Fluids—Fundamentals and Applications*, NATO Advanced Studies Institute, Series E: Applied Science, edited by E. Kiran, P. G. Debenedetti, and C. J. Peters (Kluwer, Dordrecht, 2000), Vol. 366.
- [9] R. Riehn and R. H. Austin, *Anal. Chem.* **78**, 5933 (2006).
- [10] P. Pfeuty and G. Toulouse, *Introduction to the Renormalization Group and to Critical Phenomena* (Wiley, London, 1977).
- [11] S. Dietrich, in *Phase Transitions in Surface Films 2*, NATO Advanced Studies Institute, Series B: Physics, edited by H. Taub, G. Torzo, H. J. Lauter, and S. C. Fain, Jr. (Plenum, New York, 1991), Vol. 267, p. 391, and references therein.
- [12] D. Fenistein, D. Bonn, S. Rafai, G. H. Wegdam, J. Meunier, A. O. Parry, and M. M. Telo da Gama, *Phys. Rev. Lett.* **89**, 096101 (2002).
- [13] J. Bowers, A. Zarbakhsh, A. Querol, H. K. Christenson, I. A. McLure, and R. Cubitt, *J. Chem. Phys.* **121**, 9058 (2004).
- [14] P. Tarazona, M. M. Telo da Gama, and M. Robert, *J. Chem. Phys.* **86**, 1521 (1987).
- [15] M. M. Telo da Gama and U. Marini Bettolo Marconi, *Physica A* **171**, 69 (1991).

- [16] S. Fisk and B. Widom, *J. Chem. Phys.* **50**, 3219 (1969).
- [17] J. R. Silvius, *Thermotropic Phase Transitions of Pure Lipids in Model Membranes and Their Modifications by Membrane Proteins* (Wiley, New York, 1982).
- [18] A. R. Honerkamp-Smith, P. Cicuta, M. D. Collins, S. L. Veatch, M. den Nijs, M. Schick, and S. L. Keller, *Biophys. J.* **95**, 236 (2008).
- [19] D. B. Abraham, *Phys. Rev. Lett.* **44**, 1165 (1980).
- [20] A. Maciołek, A. Ciach, and R. Evans, *J. Chem. Phys.* **108**, 9765 (1998); A. Ciach, A. Maciołek, and J. Stecki, *ibid.* **108**, 5913 (1998).
- [21] S. R. White, *Phys. Rev. Lett.* **69**, 2863 (1992); S. R. White, *Phys. Rev. B* **48**, 10345 (1993).
- [22] T. Nishino, *J. Phys. Soc. Jpn.* **64**, 3598 (1995).
- [23] *Density-Matrix Renormalization. A New Numerical Method in Physics*, Lecture Notes in Physics Vol. 528, edited by I. Peschel, X. Wang, M. Kaulke, and K. Hallberg (Springer, Berlin, 1999).
- [24] U. Schollwöck, *Rev. Mod. Phys.* **77**, 259 (2005).
- [25] (a) A. Maciołek, A. Ciach, and A. Drzewiński, *Phys. Rev. E* **60**, 2887 (1999); (b) **64**, 026123 (2001); (c) A. Drzewiński, A. Maciołek, and A. Ciach, *ibid.* **61**, 5009 (2000); (d) A. Maciołek, A. Drzewiński, and R. Evans, *ibid.* **64**, 056137 (2001).
- [26] A. Drzewiński and K. Szota, *Phys. Rev. E* **71**, 056110 (2005); A. Drzewiński, A. O. Parry, and K. Szota, *ibid.* **75**, 041110 (2007).
- [27] A. Drzewiński, A. Maciołek, A. Barasiński, and S. Dietrich, preceding paper, *Phys. Rev. E* **79**, 041144 (2009).
- [28] D. Beysens and D. Estève, *Phys. Rev. Lett.* **54**, 2123 (1985); B. M. Law, J.-M. Petit, and D. Beysens, *Phys. Rev. E* **57**, 5782 (1998).
- [29] H. Guo, T. Narayanan, M. Sztuchi, P. Schall, and G. H. Wegdam, *Phys. Rev. Lett.* **100**, 188303 (2008).
- [30] M. Schick, in *Liquids at Interfaces*, Proceedings of the Les Houches Summer School in Theoretical Physics, edited by J. Charvolin, J. F. Joanny, and J. Zinn-Justin (North-Holland, Amsterdam, 1990), p. 415.
- [31] R. Lipowsky, *Phys. Rev. B* **32**, 1731 (1985).
- [32] M. E. Fisher and P. G. de Gennes, *C. R. Seances Acad. Sci., Ser. B* **287**, 207 (1978).
- [33] G. Flöter and S. Dietrich, *Z. Phys. B: Condens. Matter* **97**, 213 (1995).
- [34] R. Pandit, M. Schick, and M. Wortis, *Phys. Rev. B* **26**, 5112 (1982).
- [35] T. Getta and S. Dietrich, *Phys. Rev. E* **47**, 1856 (1993).
- [36] V. Privman and M. E. Fisher, *J. Stat. Phys.* **33**, 385 (1983), and references therein.
- [37] K. Binder, *Annu. Rev. Mater. Res.* **38**, 123 (2008).
- [38] W. Thomson, *Philos. Mag.* **42**, 448 (1871).
- [39] L. Onsager, *Phys. Rev.* **65**, 117 (1944).
- [40] R. Evans, *J. Phys.: Condens. Matter* **2**, 8989 (1990), and references therein.
- [41] M. E. Fisher and H. Nakanishi, *J. Chem. Phys.* **75**, 5857 (1981); H. Nakanishi and M. E. Fisher, *ibid.* **78**, 3279 (1983).
- [42] K. Binder, D. Landau, and M. Müller, *J. Stat. Phys.* **110**, 1411 (2003).
- [43] A. O. Parry and R. Evans, *Phys. Rev. A* **46**, 5282 (1992).
- [44] E. Carlon, A. Drzewiński, and J. Rogiers, *Phys. Rev. B* **58**, 5070 (1998).
- [45] S. Dietrich and M. Napiórkowski, *Phys. Rev. A* **43**, 1861 (1991).
- [46] M. Napiórkowski, W. Koch, and S. Dietrich, *Phys. Rev. A* **45**, 5760 (1992).
- [47] J. Stecki, *Phys. Rev. B* **47**, 7519 (1993), and references therein.
- [48] J. Bowers, A. Zarbakhsh, I. A. McLure, J. R. P. Webster, R. Steitz, and H. K. Christenson, *J. Phys. Chem. C* **111**, 5568 (2007).